13

Nonlinear Systems of Conservation Laws

In Chapter 3 we developed the theory of *linear systems* of hyperbolic equations, in which case the general Riemann problem can be solved by decomposing the jump in states into eigenvectors of the coefficient matrix. Each eigenvector corresponds to a wave traveling at one of the characteristic speeds of the system, which are given by the corresponding eigenvalues of the coefficient matrix.

In Chapter 11 we explored *nonlinear scalar* problems, and saw that when the wave speed depends on the solution, then waves do not propagate unchanged, but in general will deform as compression waves or expansion waves, and that shock waves can form from smooth initial data. The solution to the Riemann problem (in the simplest case where the flux function is convex) then consists of a single shock wave or centered rarefaction wave.

In this chapter we will see that these two theories can be melded together into an elegant general theory for *nonlinear systems* of equations. As in the linear case, solving the Riemann problem for a system of m equations will typically require splitting the jump in states into m separate waves. Each of these waves, however, can now be a shock wave or a centered rarefaction wave.

We will develop this general theory using the one-dimensional shallow water equations as a concrete example. The same theory will later be illustrated for several other systems of equations, including the Euler equations of gas dynamics in Chapter 14. The shallow water equations are a nice example to consider first, for several reasons. It is a system of only two equations, and hence the simplest step up from the scalar case. The nonlinear structure of the equations is fairly simple, making it possible to solve the Riemann problem explicitly, and yet the structure is typical of what is seen in other important examples such as the Euler equations. Finally, it is possible to develop intuition quite easily for how solutions to the shallow water equations should behave, and even perform simple experiments illustrating some of the results we will see.

In [281] the isothermal equations are used as the primary example. This is also a simple system of two equations with a nonlinear structure very similar to that of the shallow water equations. This system is discussed briefly in Section 14.6. More details and development of the theory of nonlinear systems based on the isothermal equations may be found in [281].

13.1 The Shallow Water Equations

To derive the one-dimensional shallow water equations, we consider fluid in a channel of unit width and assume that the vertical velocity of the fluid is negligible and the horizontal velocity $u(x, t)$ is roughly constant throughout any cross section of the channel. This is true if we consider small-amplitude waves in a fluid that is shallow relative to the wavelength.

We now assume the fluid is incompressible, so the density $\bar{\rho}$ is constant. Instead we allow the depth of the fluid to vary, and it is this depth, or *height* $h(x, t)$, that we wish to determine. The total mass in $[x_1, x_2]$ at time t is

$$\int_{x_1}^{x_2} \bar{\rho} h(x, t)\, dx.$$

The density of momentum at each point is $\bar{\rho} u(x, t)$, and integrating this vertically gives the mass flux to be $\bar{\rho} u(x, t) h(x, t)$. The constant $\bar{\rho}$ drops out of the conservation-of-mass equation, which then takes the familiar form (compare (2.32))

$$h_t + (uh)_x = 0. \tag{13.1}$$

The quantity hu is often called the *discharge* in shallow water theory, since it measures the flow rate of water past a point.

The conservation-of-momentum equation also takes the same form as in gas dynamics (see (2.34)),

$$(\bar{\rho} hu)_t + (\bar{\rho} hu^2 + p)_x = 0, \tag{13.2}$$

but now p is determined from a hydrostatic law, stating that the pressure at distance $h - y$ below the surface is $\bar{\rho} g(h - y)$, where g is the gravitational constant. This pressure arises simply from the weight of the fluid above. Integrating this vertically from $y = 0$ to $y = h(x, t)$ gives the total pressure felt at (x, t), the proper pressure term in the momentum flux:

$$p = \frac{1}{2} \bar{\rho} g h^2. \tag{13.3}$$

Using this in (13.2) and canceling $\bar{\rho}$ gives

$$(hu)_t + \left(hu^2 + \frac{1}{2} g h^2 \right)_x = 0. \tag{13.4}$$

We can combine equations (13.1), (13.4) into the system of *one-dimensional shallow water equations*

$$\begin{bmatrix} h \\ hu \end{bmatrix}_t + \begin{bmatrix} uh \\ hu^2 + \frac{1}{2} g h^2 \end{bmatrix}_x = 0. \tag{13.5}$$

Note that this is equivalent to the isentropic equations of gas dynamics (discussed in Section 2.6) with the value $\gamma = 2$, since setting $P(\rho) = \frac{1}{2} g \rho^2$ in (2.38) gives the same system.

If we assume that h and u are smooth, then equation (13.4) can be simplified by expanding the derivatives and using (13.1) to replace the h_t term. Then several terms drop out, and (13.4) is reduced to

$$u_t + \left(\frac{1}{2}u^2 + gh\right)_x = 0. \tag{13.6}$$

Finally, the explicit dependence on g can be eliminated by introducing the variable $\varphi = gh$ into (13.1) and (13.6). The system then becomes

$$\begin{bmatrix} u \\ \varphi \end{bmatrix}_t + \begin{bmatrix} u^2/2 + \varphi \\ u\varphi \end{bmatrix}_x = 0. \tag{13.7}$$

This set of equations is equivalent to the previous set (13.5) for smooth solutions, but it is important to note that the manipulations performed above depend on smoothness. For problems with shock waves, the two sets of conservation laws are not equivalent, and we know from Section 12.9 that it is crucial that we use the correct set in calculating shock waves. The form (13.5), which is derived directly from the original integral equations, is the correct set to use.

Since we will be interested in studying shock waves, we use the form (13.5) and take

$$q(x,t) = \begin{bmatrix} h \\ hu \end{bmatrix} = \begin{bmatrix} q^1 \\ q^2 \end{bmatrix}, \qquad f(q) = \begin{bmatrix} hu \\ hu^2 + \frac{1}{2}gh^2 \end{bmatrix} = \begin{bmatrix} q^2 \\ (q^2)^2/q^1 + \frac{1}{2}g(q^1)^2 \end{bmatrix}.$$

For smooth solution, these equations can equivalently be written in the quasilinear form

$$q_t + f'(q)q_x = 0,$$

where the Jacobian matrix $f'(q)$ is

$$f'(q) = \begin{bmatrix} 0 & 1 \\ -(q^2/q^1)^2 + gq^1 & 2q^2/q^1 \end{bmatrix} = \begin{bmatrix} 0 & 1 \\ -u^2 + gh & 2u \end{bmatrix}. \tag{13.8}$$

The eigenvalues of $f'(q)$ are

$$\lambda^1 = u - \sqrt{gh}, \qquad \lambda^2 = u + \sqrt{gh}, \tag{13.9}$$

with the corresponding eigenvectors

$$r^1 = \begin{bmatrix} 1 \\ u - \sqrt{gh} \end{bmatrix}, \qquad r^2 = \begin{bmatrix} 1 \\ u + \sqrt{gh} \end{bmatrix}. \tag{13.10}$$

Note that the eigenvalues and eigenvectors are functions of q for this nonlinear system.

If we wish to study waves with very small amplitude, then we can linearize these equations to obtain a linear system. Suppose the fluid is essentially at a constant depth $h_0 > 0$ and moving at a constant velocity u_0 (which may be zero), and let q now represent the perturbations from this constant state, so

$$q = \begin{bmatrix} h - h_0 \\ hu - h_0u_0 \end{bmatrix} \quad \text{and} \quad q_0 = \begin{bmatrix} h_0 \\ h_0u_0 \end{bmatrix}.$$

Then expanding the flux function and dropping terms of $\mathcal{O}(\|q\|^2)$ gives the linear system $q_t + Aq_x = 0$ where $A = f'(q_0)$. Hence small-amplitude waves move at the characteristic velocities $\lambda_0^1 = u_0 - c_0$ and $\lambda_0^2 = u_0 + c_0$, where $c_0 = \sqrt{gh_0}$. These waves propagate at speed $\pm c_0$ relative to the fluid, exactly analogous to acoustic waves in a moving fluid as in Section 2.8. These shallow water waves should not be confused with sound waves, however. Sound does propagate in water, due to its slight compressibility, but in the shallow water equations we are ignoring this compressibility and hence ignoring sound waves. The waves we are modeling are often called *gravity waves*, since they are driven by the hydrostatic pressure resulting from gravity. They typically propagate at a speed $\sqrt{gh}$ that is much less than the speed of sound in water.

Note that λ^1 and λ^2 can be of either sign, depending on the magnitude of u relative to c. In shallow water theory the ratio

$$Fr = |u|/c \tag{13.11}$$

is called the *Froude number*, and is analogous to the Mach number of gas dynamics.

The wave speed $\sqrt{gh_0}$ depends on the depth of the fluid; waves in deeper water move faster. Note that within a wave the depth of the fluid varies (it is deeper at a crest than in a trough), and so we should expect the crest of a wave to propagate slightly faster than a trough. If the amplitude of the wave is very small compared to h_0, then we can safely ignore this slight variation in speed, which is what we do in linearizing the equations. Then all parts of the wave travel at the same speed based on the background depth h_0, and the wave propagates with its shape unchanged. For waves with larger amplitude, however, the deformation of the wave due to differing wave speeds may be quite noticeable. In this case the linearized equations will not be an adequate model and the full nonlinear equations must be solved.

The nonlinear distortion of a wave leads to a steepening of the wave in the region where the fast-moving crest is catching up with the slower trough ahead of it (a compression wave), and a flattening of the wave (an expansion or rarefaction) in the region where the crest is pulling away from the following trough. This is similar to what is illustrated in Figure 11.1 for the nonlinear equations of traffic flow.

This behavior is familiar from watching waves break on the beach. Far from shore the waves we normally observe have a wavelength that is very small compared to the water depth, and hence they are governed by surface-wave theory rather than shallow water theory. Near the beach, however, the water depth is small enough that nonlinear shallow water theory applies. In this shallow water, the difference in h between crests and troughs is significant and the waves steepen. In fact the crest is often observed to move beyond the position of the preceding trough, somewhat like what is shown in Figure 11.4(b). At this point the assumptions of shallow water theory no longer hold, and a more complicated set of equations would have to be used to model *breakers*. Beyond the breaking time the depth h is triple-valued, a situation that obviously can't occur with other systems of conservation laws (such as traffic flow or gas dynamics) where the corresponding variable is a density that must be single-valued.

This extreme behavior of breaking waves results from the additional complication of a sloping beach. This leads to a continuous decrease in the fluid depth seen by the wave and a severe accentuation of the nonlinear effects. (The sloping beach, or more generally any

variation in the bottom topography, also leads to additional source terms in the shallow water equations.) Shallow water waves in a domain with a flat bottom will typically not exhibit this type of breakers. Instead the gradual steepening of the wave due to nonlinearity would be counterbalanced by other effects such as surface tension (and also the vertical velocity, which is ignored in the one-dimensional model). Modeling these other effects would lead to higher-order derivatives in the equations (with small coefficients) and consequently the equations would have smooth solutions for all time, analogous to what is seen in Figure 11.6 for the viscous scalar equation. When these coefficients are small, the wave can become nearly discontinuous, and the shock-wave solution to the hyperbolic system gives a good approximation to such solutions. In shallow water flow, a shock wave is often called a *hydraulic jump*.

Example 13.1. Figure 13.1 shows the evolution of a hump of water (with initial velocity 0). As with the acoustics equations (see Figure 3.1), the hump gives rise to two waves, one moving in each direction. If the height of the hump were very small compared to the

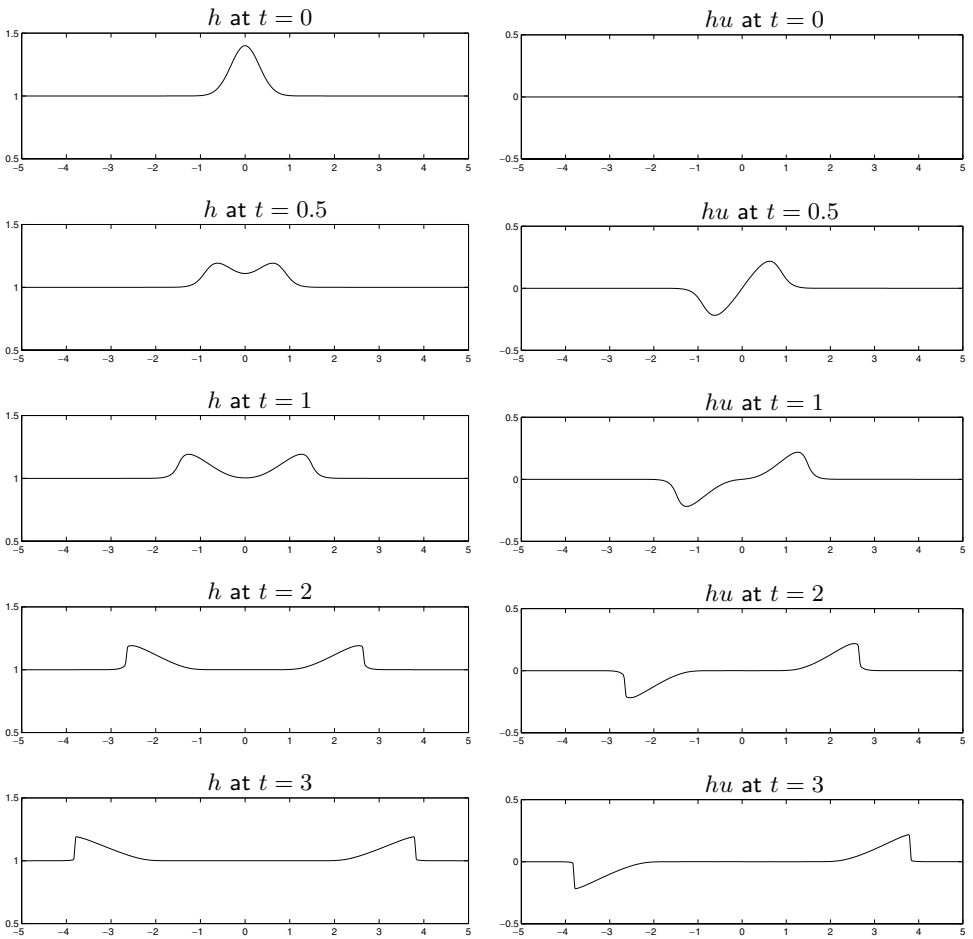

Fig. 13.1. Evolution of an initial depth perturbation, concentrated near the origin, into left-going and right-going waves. The shallow water equations are solved with $g = 1$. The left column shows the depth $q^1 = h$, the right column shows the momentum $q^2 = hu$. `[claw/book/chap13/swhump]`

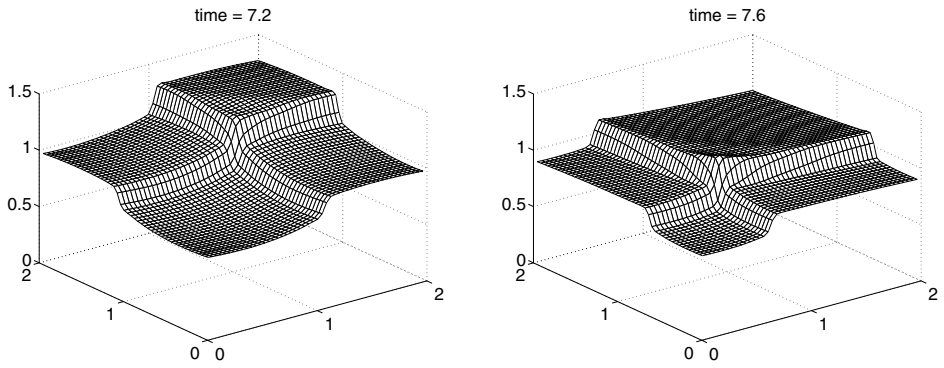

Fig. 13.2. Shallow water sloshing in a rectangular pan that is oscillated along the diagonal. [claw/book/chap13/slosh]

background depth $h_0 = 1$, then these would propagate with their shape essentially unchanged, at the characteristic speeds $\pm\sqrt{gh_0} = 1$. In Figure 13.1 the variation in depth is sufficiently large that the nonlinearity plays a clear role, and each wave shows the same behavior as the nonlinear traffic-flow example of Figure 11.1. The front of the wave (relative to its direction of motion) steepens through a compression wave into a shock, while the back spreads out as a rarefaction wave.

Example 13.2. One can experiment with shock waves in shallow water by putting a little water into a shallow rectangular pan and adding some food coloring to make the waves more visible. Oscillate the pan slowly along one axis and you should be able to excite a single "shock wave" propagating back and forth in the dish. Oscillate the dish along the diagonal and a pair of waves will be excited as shown in Figure 13.2.

Example 13.3. A stationary shock wave of the sort shown in Figure 13.3 is easily viewed in the kitchen sink. Turn on the faucet and hold a plate in the stream of water, a few inches below the faucet. You should see a roughly circular region on the surface of the plate where the water flows very rapidly outwards away from the stream in a very thin layer. This

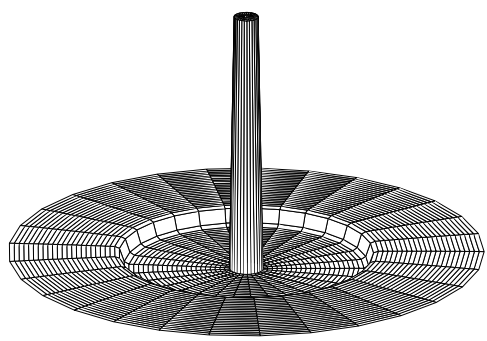

Fig. 13.3. Cartoon of water coming out of a faucet and hitting a horizontal surface such as the sink. The water expands outwards in a thin layer that suddenly thickens through a hydraulic jump (stationary shock wave).

region is bounded by a hydraulic jump, where the depth of the water suddenly increases and its speed abruptly decreases. By adjusting the flow rate or angle of the plate you should be able to make the location of this shock wave move around. When the conditions are fixed, the shock is stationary and has zero propagation speed. This can be modeled by the two-dimensional shallow water equations, or in the radially symmetric case by the one-dimensional equations with additional source terms incorporated to model the geometric effects as described in Section 18.9.

13.2 Dam-Break and Riemann Problems

Consider the shallow water equations (13.5) with the piecewise-constant initial data

$$h(x,0) = \begin{cases} h_l & \text{if } x < 0, \\ h_r & \text{if } x > 0, \end{cases} \qquad u(x,0) = 0, \tag{13.12}$$

where $h_l > h_r \geq 0$. This is a special case of the Riemann problem in which $u_l = u_r = 0$, and is called the *dam-break problem* because it models what happens if a dam separating two levels of water bursts at time $t = 0$. This is the shallow water equivalent of the shock-tube problem of gas dynamics (Section 14.13). We assume $h_r > 0$.

Example 13.4. Figure 13.4 shows the evolution of the depth and fluid velocity for the dam-break problem with data $h_l = 3$ and $h_r = 1$. Figure 13.5 shows the structure of this solution in the x–t plane. Water flows from left to right in a wedge that expands from the dam location $x = 0$. At the right edge of this wedge, moving water with some intermediate depth h_m and velocity $u_m > 0$ slams into the stationary water with $h = h_r$, accelerating it instantaneously

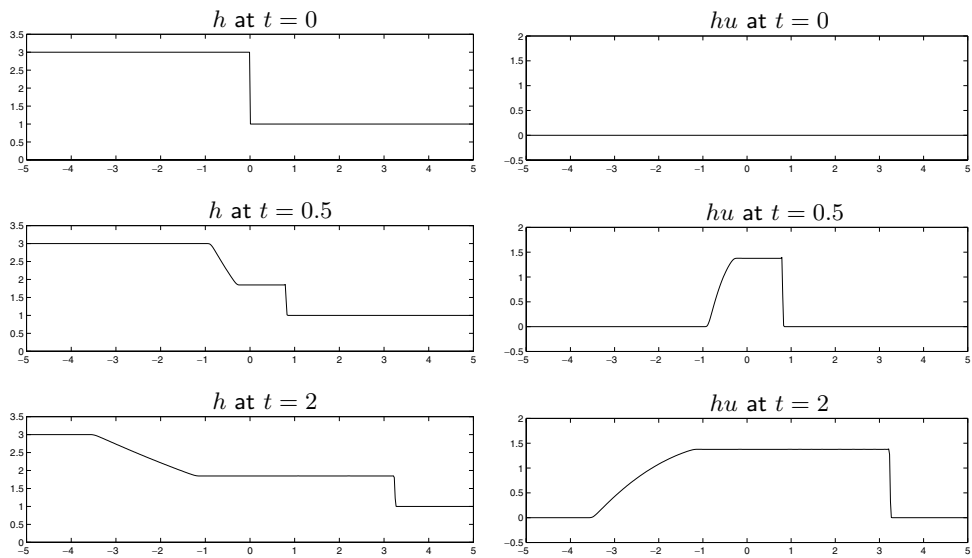

Fig. 13.4. Solution of the dam-break Riemann problem for the shallow water equations with $u_l = u_r = 0$. On the left is the depth h and on the right is the momentum hu. `[claw/book/chap13/dambreak]`

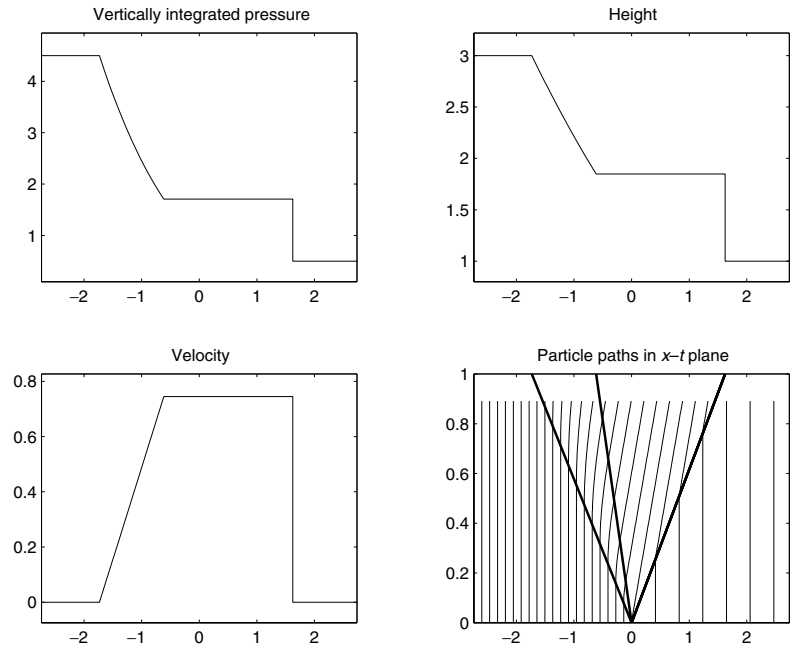

Fig. 13.5. Structure of the similarity solution of the dam-break Riemann problem for the shallow water equations with $u_l = u_r = 0$. The depth h, velocity u, and vertically integrated pressure are displayed as functions of x/t. The structure in the x–t plane is also shown with particle paths indicated for a set of particles with the spacing between particles inversely proportional to the depth. `[claw/book/chap13/rpsoln]`

through a shock wave. This is roughly analogous to the traffic-jam shock wave studied in Section 11.1. On the left edge, the water is accelerated away from the deeper stationary water through the structure of a centered rarefaction wave, analogous to the accelerating traffic situation of Section 11.1. For the scalar traffic flow model, we observed *either* a shock wave *or* a rarefaction wave as the Riemann solution, depending on the particular data. The shallow water equations are a system of two equations, and so the Riemann solution contains two waves. For the case of the dam-break problem ($u_l = u_r = 0$), these always consist of one shock and one rarefaction wave.

Figure 13.5 shows the structure of the exact similarity solution of this Riemann problem, along with particle paths in x–t plane. Note that the fluid is accelerated smoothly through the rarefaction wave and abruptly through the shock. The formulas for this solution will be worked out in Section 13.9 after developing the necessary background.

13.3 Characteristic Structure

Figure 13.6 shows the characteristic structure of the dam-break problem with data (13.12) in the case $h_l > h_r$. Figure 13.6(a) shows typical characteristic curves satisfying $dX/dt = \lambda^1 = u - \sqrt{gh}$ (called 1-characteristics), while Figure 13.6(b) shows the 2-characteristic curves satisfying $dX/dt = \lambda^2 = u + \sqrt{gh}$. Note that each characteristic direction is constant (the curves are straight lines) in each wedge where q is constant.

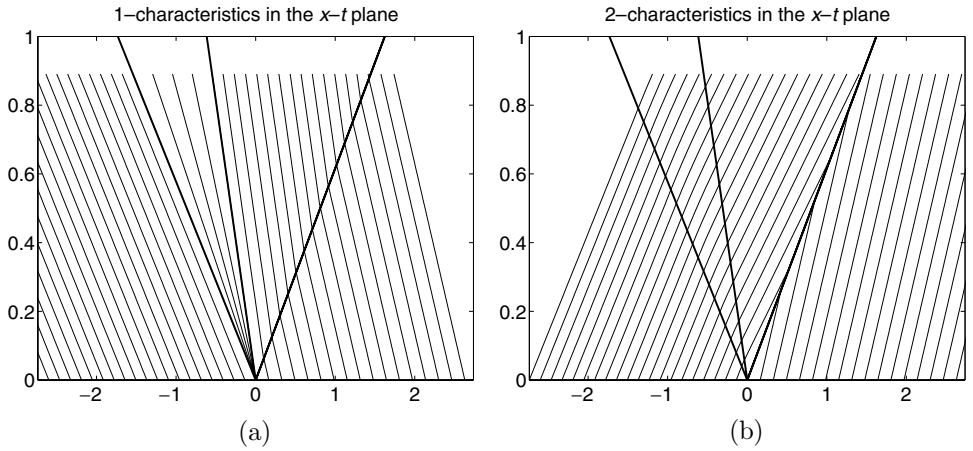

Fig. 13.6. Solution of the dam-break Riemann problem for the shallow water equations, shown in the x–t plane. The dark lines show the shock wave and the edges of the rarefaction wave seen in Figure 13.4. The lighter lines show 1-characteristics and 2-characteristics.

In Figure 13.6(a) we see that the 1-characteristics behave near the 1-rarefaction wave just as we would expect from the nonlinear scalar case. They spread out through the rarefaction wave, and the edges of this wave move with the characteristic velocity in each constant region bounding the rarefaction. Also note that the 1-characteristics *cross* the 2-waves in the sense that they are approaching the 2-wave on one side (for smaller time t) and then moving away from the 2-wave on the other side, for larger t.

On the other hand, 2-characteristics shown in Figure 13.6(b) *impinge* on the 2-shock, again as we would expect from the scalar theory. These characteristics *cross* the 1-rarefaction with a smooth change in velocity.

This is the standard situation for many nonlinear systems of equations. For a system of m equations, there will be m characteristic families and m waves in the solution to the Riemann problem. If the pth wave is a shock, then characteristics of families 1 through $p-1$ will cross the shock from left to right, characteristics of family $p+1$ through m will cross from right to left, and characteristics of family p will impinge on the shock from both sides. This classical situation is observed in many physical problems, including the Euler equations of gas dynamics, and is the case that is best understood mathematically. Such shocks are often called *classical Lax shocks*, because much of this theory was developed by Peter Lax.

In order for the classical situation to occur, certain conditions must be satisfied by the flux function $f(q)$. We assume the system is *strictly hyperbolic*, so the eigenvalues are always distinct. The conditions of *genuine nonlinearity* must also be satisfied, analogous to the convexity condition for scalar equations. This as discussed further in Section 13.8.4. Otherwise the Riemann solution can be more complicated. As in the nonconvex scalar case discussed in Section 16.1, there can be compound waves in some family consisting of more than a single shock or rarefaction. For systems it could also happen that the number of characteristics impinging on a shock is different from what has just been described, and the shock is *overcompressive* or *undercompressive*. See Section 16.2 for further discussion.

13.4 A Two-Shock Riemann Solution

The shallow water equations are genuinely nonlinear, and so the Riemann problem always consists of two waves, each of which is a shock or rarefaction. In Example 13.4 the solution consists of one of each. The following example shows that other combinations are possible.

Example 13.5. Consider the Riemann data

$$h(x,0) \equiv h_0, \qquad u(x,0) = \begin{cases} u_l & \text{if } x < 0, \\ -u_l & \text{if } x > 0. \end{cases} \tag{13.13}$$

If $u_l > 0$, then this corresponds to two streams of water slamming into each other, with the resulting solution shown in Figure 13.7 for the case $h_0 = 1$ and $u_l = 1$. The solution is symmetric in x with $h(-x,t) = h(x,t)$ and $u(-x,t) = -u(x,t)$ at all times. A shock wave moves in each direction, bringing the fluid to rest, since the middle state must have $u_m = 0$ by symmetry. The solution to this problem is computed in Section 13.7.1.

The characteristic structure of this solution is shown in Figure 13.8. Note again that 1-characteristics impinge on the 1-shock while crossing the 2-shock, whereas 2-characteristics impinge on the 2-shock.

Note that if we look at only half of the domain, say $x < 0$, then we obtain the solution to the problem of shallow water flowing into a wall located at $x = 0$ with velocity u_l. A shock wave moves out from the wall, behind which the fluid is at rest. This is now exactly analogous to traffic approaching a red light, as shown in Figure 11.2.

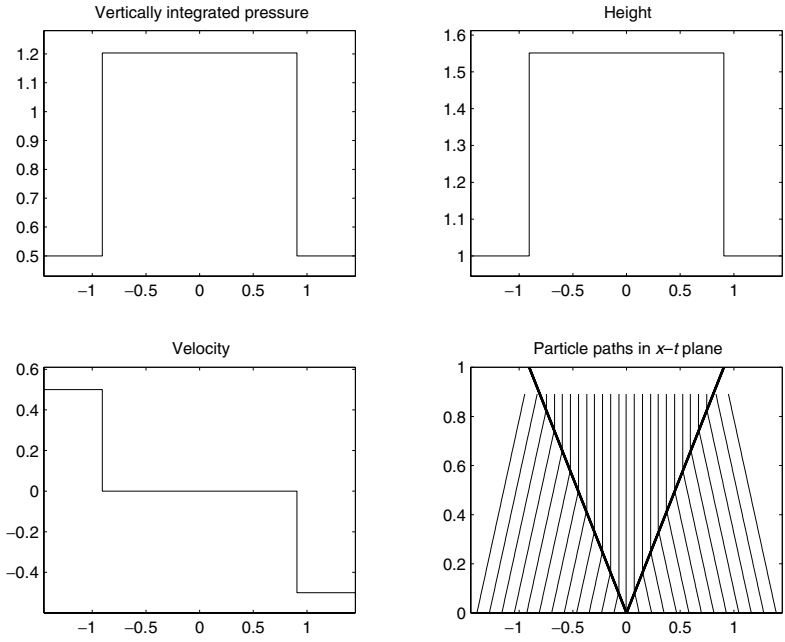

Fig. 13.7. Structure of the similarity solution of the two-shock Riemann problem for the shallow water equations with $u_l = -u_r$. The depth h, velocity u, and vertically integrated pressure are displayed as functions of x/t. The structure in the x–t plane is also shown with particle paths indicated for a set of particles with the spacing between particles inversely proportional to the depth. `[claw/book/chap13/twoshock]`

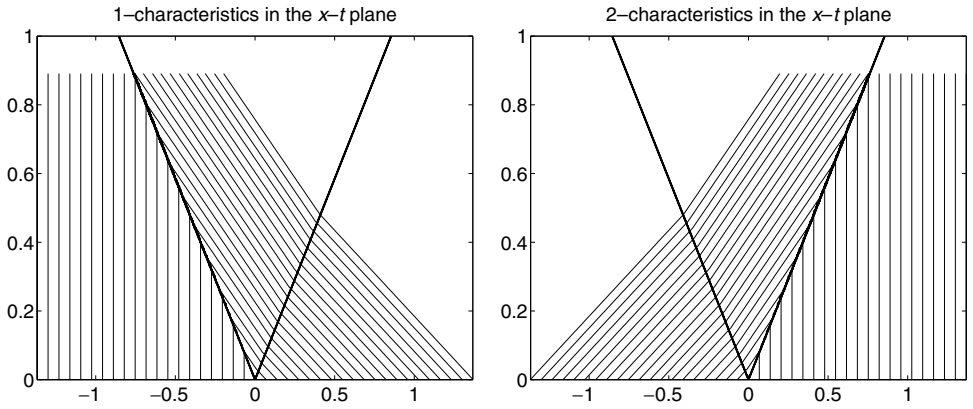

Fig. 13.8. Solution of the two-shock Riemann problem for the shallow water equations, shown in the x–t plane. The dark lines show the shocks. The lighter lines show 1-characteristics and 2-characteristics.

13.5 Weak Waves and the Linearized Problem

To understand the characteristic structure of the shallow water equations, it is useful to consider what happens in the solution to the Riemann problems discussed above in the case where the initial jump is so small that the linearized equation gives a good model. Consider the data (13.12), for example, with $h_l = h_0 + \epsilon$ and $h_r = h_0 - \epsilon$ for some $\epsilon \ll h_0$. Then if we solve the Riemann problem for the linearized equation with $u_0 = 0$ in (13.8), we find that the solution consists of two *acoustic* waves with speeds $\pm\sqrt{gh_0}$, separated by a state (h_m, u_m) with

$$h_m = h_0, \qquad u_m = \epsilon\sqrt{gh_0}.$$

The solution consists of two discontinuities. If we solved the nonlinear equations with this same data, the solution would look quite similar, but the left-going wave would be a weak rarefaction wave, spreading very slightly with time, and with the 1-characteristics spreading slightly apart rather than being parallel as in the linear problem. The right-going wave would be a weak shock wave, with slightly converging characteristics.

13.6 Strategy for Solving the Riemann Problem

Above we have presented a few specific examples of Riemann solutions for the shallow water equations. In order to apply Riemann-solver-based finite volume methods, we must be able to solve the general Riemann problem with arbitrary left and right states q_l and q_r. To compute the exact solution, we must do the following:

1. Determine whether each of the two waves is a shock or a rarefaction wave (perhaps using an appropriate entropy condition).
2. Determine the intermediate state q_m between the two waves.
3. Determine the structure of the solution through any rarefaction waves.

The first and third of these are similar to what must be done for a nonlinear scalar equation, while the second step corresponds to the procedure for solving the Riemann problem for

a linear system, in which the Rankine–Hugoniot jump relations must be used to split the jump $q_r - q_l$ into a set of allowable waves. In the next few chapters we will explore each of the necessary ingredients in more detail.

In practical finite volume methods, this process is often simplified by using an *approximate Riemann solver* as discussed in Section 15.3. Computing the exact Riemann solution can be expensive, and often excellent computational results are obtained with suitable approximations.

13.7 Shock Waves and Hugoniot Loci

In this section we begin this process by studying an isolated shock wave separating two constant states. We will determine the relation that must hold across such a shock and its speed of propagation. For an arbitrary fixed state we will determine the set of all other states that could be connected to this one by a shock of a given family. This is a necessary ingredient in order to solve a general Riemann problem.

We will continue to use the shallow water equations as the primary example system. Consider, for example, a shallow water 2-shock such as the right-going shock of Example 13.4 or Example 13.5. This shock connects some state q_m to the right state q_r from the Riemann data. We will view q_r as being fixed and determine all possible states q that can be connected to q_r by a 2-shock. We will find that there is a one-parameter family of such states, which trace out a curve in state space as shown in Figure 13.9(b). Here the state space (phase plane) is the h–hu plane. This set of states is called a *Hugoniot locus*.

Which one of these possible states corresponds to q_m in the solution to the Riemann problem depends not only on q_r but also on q_l. The state q_m must lie on the curve shown in Figure 13.9(b), but it must also lie on an analogous curve of all states that can be connected to q_l by a 1-wave, as determined below. This is completely analogous to the manner in which the linear Riemann problem was solved in Chapter 3.

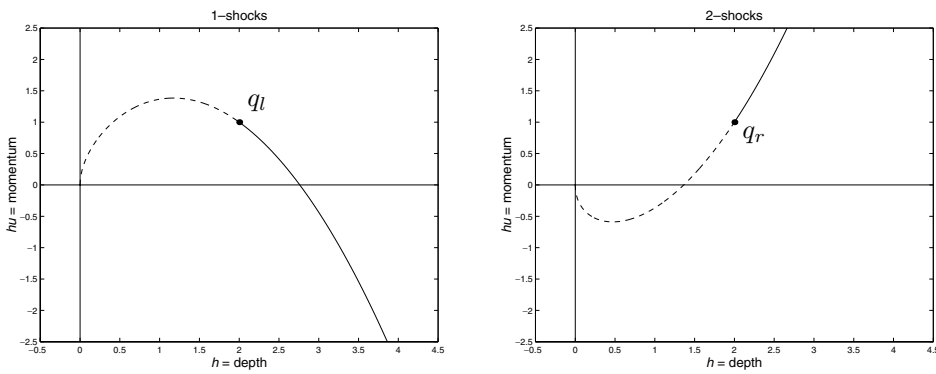

(a) (b)

Fig. 13.9. (a) Hugoniot locus of points q in shallow water state space that can be connected to a given state q_l by a 1-shock satisfying the Rankine–Hugoniot conditions. Only some of these states (on the solid portion of the curves) satisfy the entropy condition; see Section 13.7.2. (b) Hugoniot locus of points in shallow water state space that can be connected to a given state q_r by a 2-shock satisfying the Rankine–Hugoniot conditions (13.15).

We now consider the problem of determining all states q that can be connected to some fixed state q_* (representing either q_l or q_r) by a shock. Recall from Section 11.8 that across any shock the Rankine–Hugoniot condition (11.20) must be satisfied, so

$$s(q_* - q) = f(q_*) - f(q). \tag{13.14}$$

For the shallow water equations, this gives a system of two equations that must simultaneously be satisfied:

$$\begin{aligned} s(h_* - h) &= h_* u_* - hu, \\ s(h_* u_* - hu) &= h_* u_*^2 - hu^2 + \frac{1}{2} g(h_*^2 - h^2). \end{aligned} \tag{13.15}$$

Recall that (h_*, u_*) is fixed and we wish to find all states (h, u) and corresponding speeds s satisfying these relations. We thus have two equations with three unknowns, so we expect to find a one-parameter family of solutions. In fact there are two distinct families of solutions, corresponding to 1-shocks and 2-shocks. For the time being we use the term "shock" to refer to a discontinuous weak solution satisfying the Rankine–Hugoniot condition. Later we will consider the additional admissibility condition that is required to ensure that such a solution is truly a physical shock wave.

There are many different ways to parameterize these families. Fairly simple formulas result from using h as the parameter. For each value of h we will determine the corresponding u and s, and plotting hu against h will give the curves shown in Figure 13.9.

We first determine u by eliminating s from the system (13.15). The first equation gives

$$s = \frac{h_* u_* - hu}{h_* - h}, \tag{13.16}$$

and substituting this into the second equation gives an equation relating u to h. This is a quadratic equation in u that, after simplifying somewhat, becomes

$$u^2 - 2u_* u + \left[u_*^2 - \frac{g}{2} \left(\frac{h_*}{h} - \frac{h}{h_*} \right) (h_* - h) \right] = 0,$$

with roots

$$u(h) = u_* \pm \sqrt{\frac{g}{2} \left(\frac{h_*}{h} - \frac{h}{h_*} \right) (h_* - h)}. \tag{13.17}$$

Note that when $h = h_*$ this reduces to $u = u_*$, as we expect, since the curves we seek must pass through the point (h_*, u_*).

For each $h \neq h_*$ there are two different values of u, corresponding to the two families of shocks. In the case of a very weak shock ($q \approx q_*$) we expect the linearized theory to hold, and so we expect one of these curves to be tangent to the eigenvector $r^1(q_*)$ at q_* and the other to be tangent to $r^2(q_*)$. This allows us to distinguish which curve corresponds to the 1-shocks and which to 2-shocks. To see this more clearly, we multiply (13.17) by h and reparameterize by a value α, with

$$h = h_* + \alpha,$$

so that $h = h_*$ at $\alpha = 0$, to obtain

$$hu = h_* u_* + \alpha \left[u_* \pm \sqrt{g h_* \left(1 + \frac{\alpha}{h_*}\right)\left(1 + \frac{\alpha}{2h_*}\right)} \right]. \tag{13.18}$$

Hence we have

$$q = q_* + \alpha \begin{bmatrix} 1 \\ u_* \pm \sqrt{g h_* + \mathcal{O}(\alpha)} \end{bmatrix} \quad \text{as } \alpha \to 0.$$

For α very small (as q approaches q_*), we can ignore the $\mathcal{O}(\alpha)$ term and we see that these curves approach the point q_* tangent to the vectors

$$\begin{bmatrix} 1 \\ u_* \pm \sqrt{g h_*} \end{bmatrix},$$

which are simply the eigenvectors of the Jacobian matrix (13.8) at q_*. From this we see that choosing the $-$ sign in (13.18) gives the locus of 1-shocks, while the $+$ sign gives the locus of 2-shocks. (Note: The same is not true in (13.17), where choosing a single sign gives part of one locus and part of the other as h varies.)

13.7.1 The All-Shock Riemann Solution

Now consider a general Riemann problem with data q_l and q_r, and suppose we know that the solution consists of two shocks. We can then solve the Riemann problem by finding the state q_m that can be connected to q_l by a 1-shock and also to q_r by a 2-shock.

We found in the previous section that through the point q_r there is a curve of points q that can be connected to q_r by a 2-shock. For the shallow water equations, these points satisfy (13.18) with the plus sign and with $q_* = q_r$. Since q_m must lie on this curve, we have

$$h_m u_m = h_r u_r + (h_m - h_r)\left[u_r + \sqrt{g h_r \left(1 + \frac{h_m - h_r}{h_r}\right)\left(1 + \frac{h_m - h_r}{2h_r}\right)} \right],$$

which can be simplified to give

$$u_m = u_r + (h_m - h_r)\sqrt{\frac{g}{2}\left(\frac{1}{h_m} + \frac{1}{h_r}\right)}. \tag{13.19}$$

Similarly, there is a curve through q_l of states that can be connected to q_l by a 1-shock, obtained by setting $q_* = q_l$ and taking the minus sign in (13.18). Since q_m must lie on this curve, we find that

$$u_m = u_l - (h_m - h_l)\sqrt{\frac{g}{2}\left(\frac{1}{h_m} + \frac{1}{h_l}\right)}. \tag{13.20}$$

We thus have a system of two equations (13.19) and (13.20) for the two unknowns h_m and u_m. Solving this system gives the desired intermediate state in the Riemann solution. We

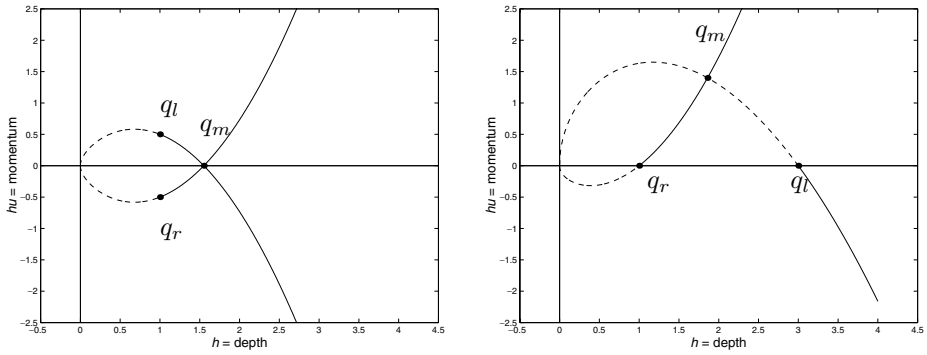

Fig. 13.10. All-shock solutions to the shallow water Riemann problem can be constructed by finding the intersection of the appropriate Hugoniot loci. (a) For Example 13.6. (b) An entropy-violating Riemann solution for Example 13.7.

can easily eliminate u_m from this system by noting that this appears only on the left of each equation, and the left-hand sides are equal, so equating the right-hand sides gives a single equation involving only the one unknown h_m. This can be solved by an iterative method for nonlinear equations, such as Newton's method.

This is analogous to solving the Riemann problem for a linear hyperbolic system, as discussed in Chapter 3, but in that case a linear system of equations results, which is more easily solved for the intermediate state.

Example 13.6. Consider the shallow water Riemann problem with $h_l = h_r = 1$, $u_l = 0.5$, and $u_r = -0.5$, as in Example 13.5. Figure 13.10(a) shows the states q_l, q_r, and q_m in the phase plane, together with the Hugoniot loci of 1-shocks through q_l and 2-shocks through q_r. In this case we could use our knowledge that $u_m = 0$ to simplify the above system further, using either (13.19) or (13.20) with the left-hand side replaced by 0. We find that the solution is $h_m = 2.1701$.

Example 13.7. What happens if we apply this same procedure to a Riemann problem where the physical solution should *not* consist of two shocks? For example, consider the dam-break Riemann problem of Example 13.4, where the solution should consist of a 1-rarefaction and a 2-shock. We can still solve the problem in terms of two "shock waves" that satisfy the Rankine–Hugoniot jump conditions, as illustrated in Figure 13.10(b). This gives a weak solution of the conservation laws, but one that does not satisfy the proper *entropy condition* for this system, as discussed in the next section. The procedure for finding the physically correct solution with a rarefaction wave is given in Section 13.9.

13.7.2 The Entropy Condition

Figure 13.6 shows the characteristic structure for the physically correct solution to the dam-break Riemann problem of Example 13.4. Figure 13.11 shows the structure for the weak solution found in Example 13.7, which consists of two discontinuities. The 1-characteristics

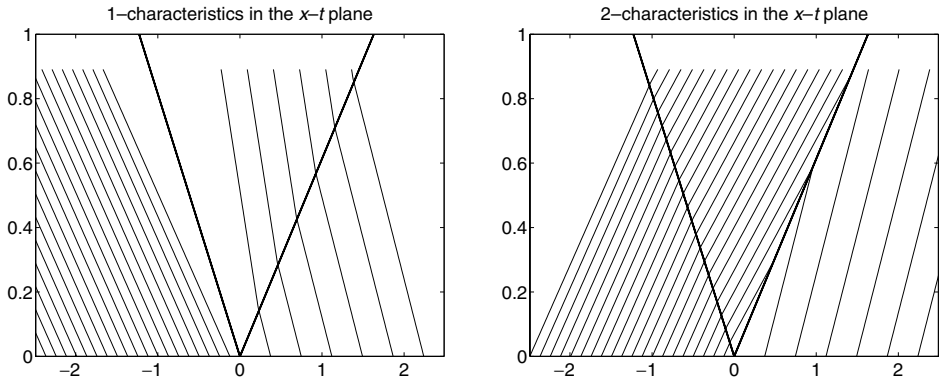

Fig. 13.11. Entropy-violating solution of the dam-break Riemann problem for the shallow water equations, shown in the x–t plane. The dark lines show the shocks. The lighter lines show 1-characteristics and 2-characteristics.

are not impinging on the 1-shock as they should, an indication that this structure is not stable to small perturbations and that this shock should be replaced by a rarefaction wave.

This suggests the following criterion for judging whether a given weak solution is in fact the physically correct solution, a generalization of the Lax Entropy Condition 11.1 to systems of equations.

Entropy Condition 13.1 (Lax). A discontinuity separating states q_l and q_r, propagating at speed s, satisfies the *Lax entropy condition* if there is an index p such that

$$\lambda^p(q_l) > s > \lambda^p(q_r), \tag{13.21}$$

so that p-characteristics are impinging on the discontinuity, while the other characteristics are crossing the discontinuity,

$$\begin{aligned} &\lambda^j(q_l) < s \quad \text{and} \quad \lambda^j(q_r) < s \qquad \text{for } j < p, \\ &\lambda^j(q_l) > s \quad \text{and} \quad \lambda^j(q_r) > s \qquad \text{for } j > p. \end{aligned} \tag{13.22}$$

In this definition we assume the eigenvalues are ordered so that $\lambda^1 < \lambda^2 < \cdots < \lambda^m$ in each state.

This condition can be shown to be correct for strictly hyperbolic conservation laws in which each field is genuinely nonlinear (as defined in Section 13.8.4). For the nonstrictly-hyperbolic case shocks may instead be overcompressive or undercompressive with a different number of characteristics impinging, as described in Section 16.2.

For the shallow water equations there is a simple criterion that can be applied to determine which parts of each Hugoniot locus give physically correct shock waves satisfying the Lax entropy condition. Across a 1-shock connecting q_l to a state q_m, we require that the characteristic velocity $\lambda^1 = u - \sqrt{gh}$ must decrease. In conjunction with the Rankine–Hugoniot condition, it can be shown that this implies that h must increase, so we require

$h_m > h_l$. Similarly, a 2-shock connecting q_m to q_r satisfies the Lax entropy condition if $h_m > h_r$. Note from Figure 13.5 and Figure 13.7 that this also means that fluid particles experience an *increase* in depth as they pass through a shock. This is similar to the physical entropy condition for gas dynamics, that gas particles must experience an increase in physical entropy as they pass through a shock wave.

Figure 13.10 shows the portions of each Hugoniot locus along which the entropy condition is satisfied as solid lines. These are simply the portions along which h is increasing. The portions indicated by dashed lines are states that can be connected by a discontinuity that satisfies the Rankine–Hugoniot condition, but not the entropy condition.

We see from Figure 13.10(b) that the solution to the dam-break Riemann problem consisting of two shocks fails to satisfy the entropy condition. Instead we must find a solution to the Riemann problem that consists of a 1-rarefaction and a 2-shock. In the next section we investigate rarefaction waves and will see that the Hugoniot locus through q_l must be replaced by a different curve, the integral curve of r^1. The intersection of this curve with the 1-shock Hugoniot locus will give the correct intermediate state q_m, as described in Section 13.9.

The shallow water equations also possess a convex entropy function $\eta(q)$; see Exercise 13.6. From this it follows that Godunov's method will converge to the physically correct solution, if the correct entropy solution to each Riemann problem is used; see Section 12.11.1.

13.8 Simple Waves and Rarefactions

Solutions to a hyperbolic system of m equations are generally quite complicated, since at any point there are typically m waves passing by, moving at different speeds, and what we observe is some superposition of these waves. In the nonlinear case the waves are constantly interacting with one another as well as deforming separately, leading to problems that generally cannot be solved analytically. It is therefore essential to look for special situations in which a single wave from one of the characteristic families can be studied in isolation. A shock wave consisting of piecewise constant data (satisfying the Rankine–Hugoniot conditions across the discontinuity) is one important example that was investigated in the previous section.

In this section we will investigate solutions that are smoothly varying (rather than discontinuous) but which also have the property that they are associated with only one characteristic family of the system. Such waves are called *simple waves*. These have already been introduced for linear systems in Section 3.4. In the linear case simple waves have fixed shape and propagate with fixed speed according to a scalar advection equation. In the nonlinear case they will deform due to the nonlinearity, but their evolution can be modeled by *scalar* nonlinear equations.

In particular, the *centered rarefaction waves* that arise in the solution to Riemann problems for nonlinear systems are simple waves, but these are just one special case. They are special in that they also have the property that they are similarity solutions of the equations and are constant along every ray $x/t =$ constant. They arise naturally from Riemann problems because of the special data used, which varies only at a single point $x = 0$, and hence all

variation in the solution flows out from the point $x = t = 0$. Recall from Section 11.10 that if $q(x, t) = \tilde{q}(x/t)$ then the function $\tilde{q}(\xi)$ must satisfy (11.26),

$$f'(\tilde{q}(x/t))\,\tilde{q}'(x/t) = \left(\frac{x}{t}\right)\tilde{q}'(x/t). \tag{13.23}$$

For a scalar equation we could cancel $\tilde{q}'(x/t)$ from this equation. For a system of equations $\tilde{q}'$ is a vector and (13.23) requires that it be an eigenvector of the Jacobian matrix $f'(\tilde{q}(x/t))$ for each value of x/t. We will see how to determine this function for centered rarefaction waves and employ it in solving the Riemann problem, but first we study some more basic ideas.

Again we will concentrate on the shallow water equations to illustrate this theory. For this system of two equations we can easily draw diagrams in the two-dimensional state space that help to elucidate the theory.

13.8.1 Integral Curves

Let $\tilde{q}(\xi)$ be a smooth curve through state space parameterized by a scalar parameter ξ. We say that this curve is an *integral curve of the vector field* r^p if at each point $\tilde{q}(\xi)$ the tangent vector to the curve, $\tilde{q}'(\xi)$, is an eigenvector of $f'(\tilde{q}(\xi))$ corresponding to the eigenvalue $\lambda^p(\tilde{q}(\xi))$. If we have chosen some particular set of eigenvectors that we call $r^p(q)$, e.g., (13.10) for the shallow water equations, then $\tilde{q}'(\xi)$ must be some scalar multiple of the particular eigenvector $r^p(\tilde{q}(\xi))$,

$$\tilde{q}'(\xi) = \alpha(\xi) r^p(\tilde{q}(\xi)). \tag{13.24}$$

The value of $\alpha(\xi)$ depends on the particular parameterization of the curve and on the normalization of r^p, but the crucial idea is that the tangent to the curve is always in the direction of the appropriate eigenvector r^p evaluated at the point on the curve.

Example 13.8. Figure 13.12 shows integral curves of r^1 and r^2 for the shallow water equations of Section 13.1, for which the eigenvectors are given by (13.10). As an example of how these curves can be determined, consider r^1 and set $\alpha(\xi) \equiv 1$, which selects one particular parameterization for which the formulas are relatively simple. Then (13.24) reduces to

$$\tilde{q}'(\xi) = r^1(\tilde{q}(\xi)) = \begin{bmatrix} 1 \\ \tilde{q}^2/\tilde{q}^1 - \sqrt{g\tilde{q}^1} \end{bmatrix} \tag{13.25}$$

by using (13.10). This gives two ordinary differential equations for the two components of $\tilde{q}(\xi)$:

$$(\tilde{q}^1)' = 1 \tag{13.26}$$

and

$$(\tilde{q}^2)' = \tilde{q}^2/\tilde{q}^1 - \sqrt{g\tilde{q}^1}. \tag{13.27}$$

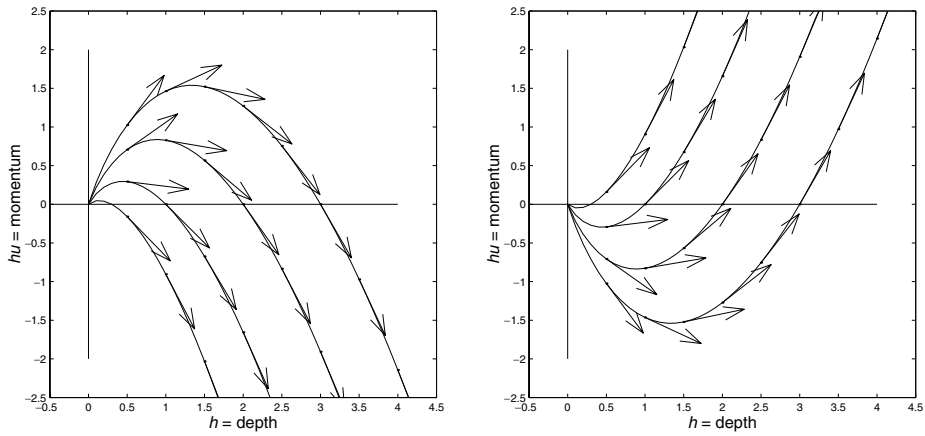

(a) (b)

Fig. 13.12. (a) Integral curves of the eigenvector field r^1 for the shallow water equations. The eigenvector $r^1(q)$ evaluated at any point on a curve is tangent to the curve at that point. (b) Integral curves for r^2.

If we set

$$\tilde{q}^1(\xi) = \xi, \tag{13.28}$$

then (13.26) is satisfied. Note that since the first component of q is h, this means we are parameterizing the integral curve by depth. With this choice of $\tilde{q}^1$, the second equation (13.27) becomes

$$(\tilde{q}^2)' = \tilde{q}^2/\xi - \sqrt{g\xi}. \tag{13.29}$$

If we fix one point (h_*, u_*) on the integral curve and require that $\tilde{q}^2(h_*) = h_* u_*$, then solving the differential equation (13.29) with this initial value yields the solution

$$\tilde{q}^2(\xi) = \xi u_* + 2\xi(\sqrt{gh_*} - \sqrt{g\xi}). \tag{13.30}$$

Plotting $(\tilde{q}^1(\xi), \tilde{q}^2(\xi))$ from (13.28) and (13.30) gives the curves shown in Figure 13.12(a). Since ξ is just the depth h, we can also state more simply that the integral curves of r^1 have the functional form

$$hu = hu_* + 2h(\sqrt{gh_*} - \sqrt{gh}). \tag{13.31}$$

In terms of the velocity instead of the momentum, we can rewrite this as

$$u = u_* + 2(\sqrt{gh_*} - \sqrt{gh}). \tag{13.32}$$

Similarly, the integral curve of r^2 passing through the point (h_*, u_*) can be shown to have the form

$$u = u_* - 2(\sqrt{gh_*} - \sqrt{gh}). \tag{13.33}$$

13.8.2 Riemann Invariants

The expression (13.32) describes an integral curve of r^1, where (h_*, u_*) is an arbitrary point on the curve. This can be rewritten as

$$u + 2\sqrt{gh} = u_* + 2\sqrt{gh_*}.$$

Since (h_*, u_*) and (h, u) are any two points on the curve, we see that the function

$$w^1(q) = u + 2\sqrt{gh} \tag{13.34}$$

has the same value at all points on this curve. This function is called a *Riemann invariant* for the 1-family, or simply a 1-Riemann invariant. It is a function of q whose value is invariant along any integral curve of r^1, though it will take a different value on a different integral curve.

Similarly, from (13.33) we see that

$$w^2(q) = u - 2\sqrt{gh} \tag{13.35}$$

is a 2-Riemann invariant, a function whose value is constant along any integral curve of r^2.

If $\tilde{q}(\xi)$ represents a parameterization of any integral curve of r^p, then since $w^p(q)$ is constant along $\tilde{q}(\xi)$ as ξ varies, we must have $\frac{d}{d\xi} w^p(\tilde{q}(\xi)) = 0$. Expanding this out gives

$$\nabla w^p(\tilde{q}(\xi)) \cdot \tilde{q}'(\xi) = 0,$$

where ∇w^p is the gradient of w^p with respect to q. By (13.24) this gives

$$\nabla w^p(\tilde{q}(\xi)) \cdot r^p(\tilde{q}(\xi)) = 0. \tag{13.36}$$

This relation must hold at any point on every integral curve, and hence in general $\nabla w^p \cdot r^p = 0$ everywhere. This gives another way to characterize a p-Riemann invariant – it is a function whose gradient is orthogonal to the eigenvector r^p at each point q.

We can also view the integral curves of r^p as being level sets of the function $w^p(q)$, so that the curves in Figure 13.12(a), for example, give a contour plot of $w^1(q)$. The gradient of $w^1(q)$ is orthogonal to the contour lines, as expressed by (13.36).

Note that all the integral curves shown in Figure 13.12 appear to meet at the origin $h = hu = 0$. This may seem odd in that they are level sets of a function w^p that takes different values on each curve. But note that each w^p involves the velocity $u = (hu)/h$, which has different limiting values depending on how the point $h = hu = 0$ is approached. The integral curves would look different if plotted in the h–u plane; see Exercise 13.2.

For a system of $m > 2$ equations, the integral curves of r^p will still be curves through the m-dimensional state space, and can be determined by solving the system (13.24) with $\alpha(\xi) \equiv 1$, for example. This is now a system of m ODEs. In general there will now be $m - 1$ distinct functions $w^p(\xi)$ that are p-Riemann invariants for each family p.

13.8.3 Simple Waves

A *simple wave* is a special solution to the conservation law in which

$$q(x,t) = \tilde{q}(\xi(x,t)), \tag{13.37}$$

where $\tilde{q}(\xi)$ traces out an integral curve of some family of eigenvectors r^p and $\xi(x,t)$ is a smooth mapping from (x,t) to the parameter ξ. This means that all states $q(x,t)$ appearing in the simple wave lie on the same integral curve. Note that any p-Riemann invariant is constant throughout the simple wave.

Of course not every function of the form (13.37) will satisfy the conservation law. The function $\xi(x,t)$ must be chosen appropriately. We compute

$$q_t = \tilde{q}'(\xi(x,t))\,\xi_t \quad \text{and} \quad q_x = \tilde{q}'(\xi(x,t))\,\xi_x,$$

so to satisfy $q_t + f(q)_x = 0$ we must have

$$\xi_t\,\tilde{q}'(\xi) + \xi_x\,f'(\tilde{q}(\xi))\,\tilde{q}'(\xi) = 0.$$

Since $\tilde{q}'(\xi)$ is always an eigenvector of $f'(\tilde{q}(\xi))$, this yields

$$[\xi_t + \xi_x \lambda^p(\tilde{q}(\xi))]\,\tilde{q}'(\xi) = 0,$$

and hence the function $\xi(x,t)$ must satisfy

$$\xi_t + \lambda^p(\tilde{q}(\xi))\,\xi_x = 0. \tag{13.38}$$

Note that this is a scalar quasilinear hyperbolic equation for ξ.

In particular, if we choose initial data $q(x,0)$ that is restricted entirely to this integral curve, so that

$$q(x,0) = \tilde{q}(\mathring{\xi}(x))$$

for some smooth choice of $\mathring{\xi}(x)$, then (13.37) will be a solution to the conservation law for $t > 0$ provided that $\xi(x,t)$ solves (13.38) with initial data $\xi(x,0) = \mathring{\xi}(x)$, at least for as long as the function $\xi(x,t)$ remains smooth. In a simple wave the nonlinear system of equations reduces to the scalar nonlinear equation (13.38) for $\xi(x,t)$.

Since (13.38) is nonlinear, the smooth solution may eventually break down at some time T_b. At this time a shock forms in $q(x,t)$ and the solution is in general no longer a simple wave for later times. States q that do not lie on the same integral curve will typically appear near the shock.

In the special case where $\lambda^p(\tilde{q}(\xi(x,0)))$ is monotonically increasing in x, the characteristics will always be spreading out and a smooth solution will exist for all time. This is a pure rarefaction wave. If the characteristic speed $\lambda^p(\tilde{q}(\xi(x,0)))$ is decreasing in x over some region, then a compression wave arises that will eventually break.

Note that $\xi(x,t)$ is constant along characteristic curves of the equation (13.38), curves $X(t)$ that satisfy $X'(t) = \lambda^p(\tilde{q}(\xi(X(t),t)))$. Since ξ is constant on this curve, so is $X'(t)$, and hence the characteristics are straight lines. Along these characteristics the value of

$q(x,t)$ is also constant, since $q(x,t)$ is determined by (13.37) and ξ is constant. Hence a simple wave behaves exactly like the solution to a scalar conservation law, as described in Chapter 11, up to the time it breaks.

For the special case of a linear hyperbolic system, simple waves satisfy scalar advection equations (λ^p is constant, independent of $\tilde{q}(\xi)$), and the theory just developed agrees with what was presented in Section 3.4.

13.8.4 Genuine Nonlinearity and Linear Degeneracy

For the shallow water equations, the characteristic speed $\lambda^p(\tilde{q}(\xi))$ varies monotonically as we move along an integral curve. We will verify this in Example 13.9, but it can be seen in Figure 13.13, where contours of λ^p are plotted along with a typical integral curve. This monotonicity is analogous to the situation for a scalar conservation law with a *convex* flux function $f(q)$, in which case the single characteristic speed $\lambda^1(q) = f'(q)$ is monotonic in q. As discussed in Section 16.1, solutions to the scalar conservation law can be considerably more complex if f is nonconvex. The same is true for systems of equations, but for many physical systems we have a property analogous to convexity. If $\lambda^p(\tilde{q}(\xi))$ varies monotonically with ξ along every integral curve, then we say that the pth field is *genuinely nonlinear*. Note that the variation of λ^p along the curve can be computed as

$$\frac{d}{d\xi}\lambda^p(\tilde{q}(\xi)) = \nabla\lambda^p(\tilde{q}(\xi)) \cdot \tilde{q}'(\xi). \tag{13.39}$$

Here $\nabla\lambda^p$ is the gradient vector obtained by differentiating the scalar $\lambda^p(q)$ with respect to each component of the vector q. The quantity in (13.39) must be nonzero everywhere if the field is to be genuinely nonlinear. If the value of (13.39) is positive, then the characteristic

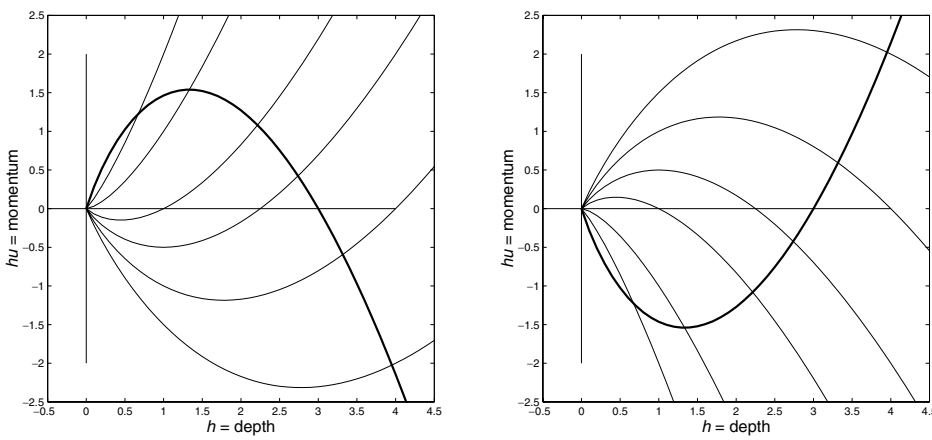

(a) (b)

Fig. 13.13. (a) A typical integral curve of the eigenvector field r^1 for the shallow water equations is shown as the heavy line. The other lines are contour lines of $\lambda^1(q)$, curves along which λ^1 is constant. The curves shown are for values $\lambda^1 = 1, 0, -1, -1.5, -2, -2.5$ from top to bottom. Note that λ^1 varies monotonically along the integral curve. (b) An integral curve for r^2 and contours of $\lambda^2(q)$ for values $\lambda^2 = 2.5, 2, 1.5, 1, 0, -1$ from top to bottom.

speed is increasing with ξ and if it is negative the speed is decreasing. If this derivative were zero at some point, then the characteristic speed would be locally constant and characteristics would be essentially parallel as in a linear problem. The property of genuine nonlinearity insures that this linear situation never occurs and characteristics are always compressing or expanding as q varies.

Since $\tilde{q}'(\xi)$ is in the direction $r^p(\tilde{q}(\xi))$ by (13.24), we see from (13.39) that the pth field is genuinely nonlinear if

$$\nabla\lambda^p(q) \cdot r^p(q) \neq 0 \tag{13.40}$$

for all q. Note that for a scalar problem $\lambda^1(q) = f'(q)$ and we can take $r^1(q) \equiv 1$, so that (13.40) reduces to the convexity requirement $f''(q) \neq 0$.

At the other extreme, in some physical systems there are characteristic fields for which the relation

$$\nabla\lambda^p(q) \cdot r^p(q) \equiv 0 \tag{13.41}$$

holds for all q. This means that λ^p is identically constant along each integral curve. A trivial example occurs in a constant-coefficient linear hyperbolic system, in which case λ^p is constant everywhere and $\nabla\lambda^p(q) \equiv 0$. But in nonlinear systems it may also happen that some field satisfies the relation (13.41) even though λ^p takes different values along different integral curves. This happens if the integral curves of r^p are identical to the contour lines of λ^p. A field satisfying (13.41) is said to be *linearly degenerate*. Through a simple wave in such a field the characteristics are parallel, as in a linear system, rather than compressing or expanding. See Section 13.12 and Section 14.9 for examples of linearly degenerate fields.

13.8.5 Centered Rarefaction Waves

A *centered rarefaction wave* is a special case of a simple wave in a genuinely nonlinear field, in which $\xi(x, t) = x/t$, so that the solution is constant on rays through the origin. A centered rarefaction wave has the form

$$q(x,t) = \begin{cases} q_l & \text{if } x/t \le \xi_1, \\ \tilde{q}(x/t) & \text{if } \xi_1 \le x/t \le \xi_2, \\ q_r & \text{if } x/t \ge \xi_2, \end{cases} \tag{13.42}$$

where q_l and q_r are two points on a single integral curve with $\lambda^p(q_l) < \lambda^p(q_r)$. This condition is required so that characteristics spread out as time advances and the rarefaction wave makes physical sense. (The picture should look like Figure 11.4(a), not Figure 11.4(b).)

For a centered rarefaction wave a particular parameterization of the integral curve is forced upon us by the fact that we set $\xi = x/t$. Rewriting this as $x = \xi t$, we see that the value $\tilde{q}(\xi)$ observed along the ray $x/t = \xi$ is propagating at speed ξ, which suggests that ξ at each point on the integral curve must be equal to the characteristic speed $\lambda^p(\tilde{q}(\xi))$ at this point. This is confirmed by noting that (13.38) in this case becomes

$$-\frac{x}{t^2} + \lambda^p(\tilde{q}(x/t))\left(\frac{1}{t}\right) = 0$$

and hence

$$\frac{x}{t} = \lambda^p(\tilde{q}(x/t)). \tag{13.43}$$

In particular, the left edge of the rarefaction fan should be the ray $x/t = \lambda^p(q_l)$ so that $\xi_1 = \lambda^p(q_l)$ in (13.42), while the right edge should be the ray $x/t = \lambda^p(q_r)$ so that $\xi_2 = \lambda^p(q_r)$. We thus have

$$\begin{aligned} \xi_1 &= \lambda^p(q_l), \qquad \tilde{q}(\xi_1) = q_l, \\ \xi_2 &= \lambda^p(q_r), \qquad \tilde{q}(\xi_2) = q_r. \end{aligned} \tag{13.44}$$

To determine how $\tilde{q}(\xi)$ varies for $\xi_1 < \xi < \xi_2$ through the rarefaction wave (13.42), rewrite (13.43) as

$$\xi = \lambda^p(\tilde{q}(\xi)) \tag{13.45}$$

and differentiate this with respect to ξ to obtain

$$1 = \nabla\lambda^p(\tilde{q}(\xi)) \cdot \tilde{q}'(\xi). \tag{13.46}$$

Using (13.24) in (13.46) gives

$$1 = \alpha(\xi)\nabla\lambda^p(\tilde{q}(\xi)) \cdot r^p(\tilde{q}(\xi)),$$

and hence

$$\alpha(\xi) = \frac{1}{\nabla\lambda^p(\tilde{q}(\xi)) \cdot r^p(\tilde{q}(\xi))}. \tag{13.47}$$

Using this in (13.24) gives a system of ODEs for $\tilde{q}(\xi)$:

$$\tilde{q}'(\xi) = \frac{r^p(\tilde{q}(\xi))}{\nabla\lambda^p(\tilde{q}(\xi)) \cdot r^p(\tilde{q}(\xi))}. \tag{13.48}$$

This system must be solved over the interval $\xi_1 \le \xi \le \xi_2$ using either of the conditions in (13.44) as an initial condition. Note that the denominator is nonzero provided that λ^p is monotonically varying. A rarefaction wave would not make sense past a point where the denominator vanishes. In particular, if the pth field is genuinely nonlinear, then the denominator is always nonzero by (13.40).

Example 13.9. For the shallow water equations we have

$$\begin{aligned} \lambda^1 &= u - \sqrt{gh} = q^2/q^1 - \sqrt{gq^1}, \\ \nabla\lambda^1 &= \begin{bmatrix} -q^2/(q^1)^2 - \frac{1}{2}\sqrt{g/q^1} \\ 1/q^1 \end{bmatrix}, \\ r^1 &= \begin{bmatrix} 1 \\ q^2/q^1 - \sqrt{gq^1} \end{bmatrix}, \end{aligned} \tag{13.49}$$

and hence

$$\nabla\lambda^1 \cdot r^1 = -\frac{3}{2}\sqrt{g/q^1}, \tag{13.50}$$

so that the equations (13.48) become

$$\tilde{q}' = -\frac{2}{3}\sqrt{\tilde{q}^1/g}\begin{bmatrix} 1 \\ \tilde{q}^2/\tilde{q}^1 - \sqrt{g\tilde{q}^1} \end{bmatrix}. \tag{13.51}$$

The first equation of this system is

$$\tilde{h}'(\xi) = -\frac{2}{3}\sqrt{\tilde{h}(\xi)/g}.$$

The general solution is

$$\tilde{h} = \frac{1}{9g}(A - \xi)^2, \tag{13.52}$$

for some constant A. This constant must be chosen so that (13.44) is satisfied, i.e., so that $\tilde{h} = h_l$ at $\xi = u_l - \sqrt{gh_l}$ and also $\tilde{h} = h_r$ at $\xi = u_r - \sqrt{gh_r}$. Provided that q_l and q_r both lie on an integral curve of r^1, as they must if they can be joined by a centered rarefaction wave, we can satisfy both of these conditions by taking

$$A = u_l + 2\sqrt{gh_l} = u_r + 2\sqrt{gh_r}. \tag{13.53}$$

Recall that $u + 2\sqrt{gh}$ is a 1-Riemann invariant, which has the same value at all points on the integral curve. We see that $\tilde{h}$ varies quadratically with $\xi = x/t$ through a rarefaction wave (13.42).

Once we know h as a function of ξ, we can use the formula (13.33), which holds through any simple wave, to determine how u varies through the rarefaction wave. (i.e., we use the fact that the Riemann invariant is constant). Note that since we know the relation between h and u from having previously found the Riemann invariants, we do not need to solve both the ODEs in the system (13.51). We have chosen the simpler one to solve. This trick is often useful for other systems as well.

Note that (13.50) is nonzero for all physically meaningful states $q^1 = h > 0$, showing that this field is genuinely nonlinear. The expressions for the 2-characteristic field are very similar (with only a few minus signs changed), and this field is also genuinely nonlinear; see Exercise 13.3.

13.8.6 The All-Rarefaction Riemann Solution

Now suppose we wish to solve a Riemann problem for which we know the solution consists of two rarefaction waves, as in the following example.

Example 13.10. Again consider the Riemann problem for the shallow water equations with data (13.13), but now take $u_l < 0$. This corresponds to two streams of water that are moving apart from one another. Again the solution will be symmetric but will consist of

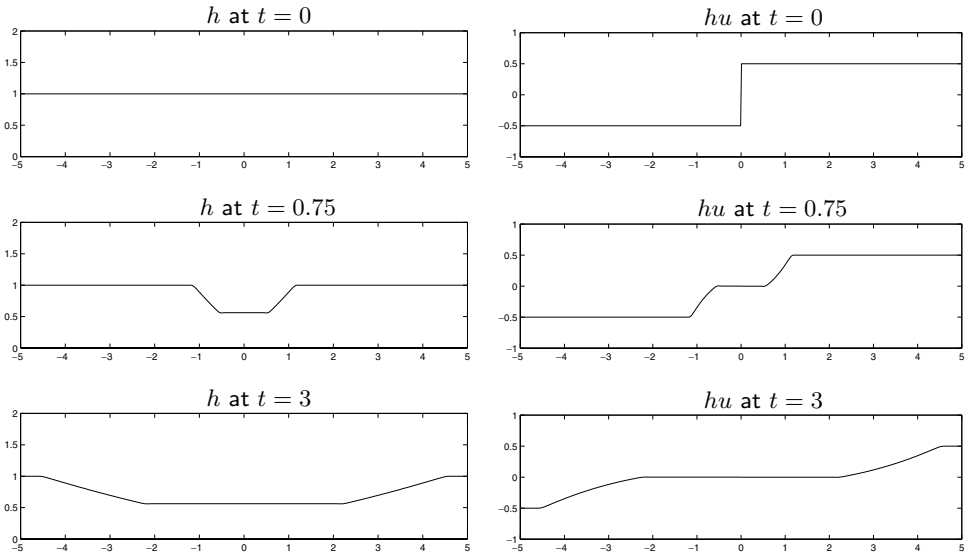

Fig. 13.14. Solution of the Riemann problem for the shallow water equations with $u_l = -u_r < 0$. `[claw/book/chap13/tworaref]`

two rarefaction waves as shown in Figure 13.14. (Looking at only half the domain gives the solution to the boundary-value problem with water flowing away from a wall.)

To solve this Riemann problem, we can proceed in a manner similar to what we did in Section 13.7.1 for the all-shock solution. There is an integral curve of r^1 through q_l consisting of all states that can be connected to q_l by a 1-rarefaction, and an integral curve of r^2 through q_r consisting of all states that can be connected to q_r by a 2-rarefaction. These are illustrated in Figure 13.15(a) for the Riemann data

$$u_l = -0.5, \quad u_r = 0.5, \quad \text{and} \quad h_l = h_r = 1. \tag{13.54}$$

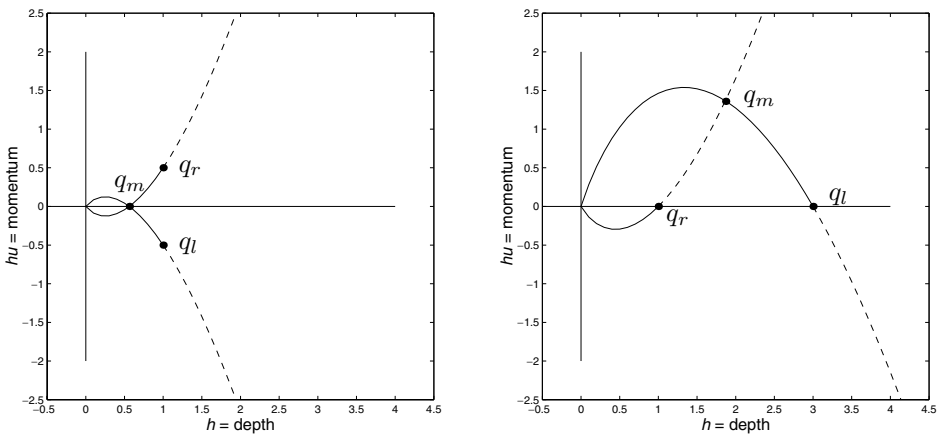

Fig. 13.15. (a) Construction of the all-rarefaction Riemann solution for the problem of Example 13.5. (b) The physically incorrect all-rarefaction Riemann solution for the dam-break problem of Example 13.4.

The intermediate state q_m in the Riemann solution must lie on both of these curves, and hence is at the intersection as shown in Figure 13.15(a). For this particular example q_m lies on the h-axis due to symmetry. In general we can find the intersection by using the fact that q_m must lie on the curve described by (13.32) with $q_* = q_l$ and on the curve described by (13.33) with $q_* = q_r$, so

$$\begin{aligned} u_m &= u_l + 2(\sqrt{gh_l} - \sqrt{gh_m}), \\ u_m &= u_r - 2(\sqrt{gh_r} - \sqrt{gh_m}). \end{aligned} \tag{13.55}$$

This is a system of two nonlinear equations for h_m and u_m. Equating the right-hand sides gives a single equation for h_m, which can be explicitly solved to obtain

$$h_m = \frac{1}{16g}[u_l - u_r + 2(\sqrt{gh_l} + \sqrt{gh_r})]^2. \tag{13.56}$$

This is valid provided that the expression being squared is nonnegative. When it reaches zero, the outflow is sufficiently great that the depth h_m goes to zero. (See Exercise 13.2.)

For the symmetric data (13.54) used in Figures 13.14 and 13.15(a), the expression (13.56) gives $h_m = (4\sqrt{g}-1)^2/16g = 9/16$, since we use $g = 1$. Then either equation from (13.55) gives $u_m = 0$.

The integral curves in Figure 13.15(a) are shown partly as dashed lines. For a given state q_l only some points on the integral curve of r^1 can be connected to q_l by a rarefaction wave that makes physical sense, since we are assuming q_l is the state on the *left* of the rarefaction wave. We must have $\lambda^1(q_l) < \lambda^1(q)$ for all states q in the rarefaction wave, and hence q must lie on the portion of the integral curve shown as a solid line (see Figure 13.13(a)). Similarly, if q_r is the state to the right of a 2-rarefaction, then states q in the rarefaction must satisfy $\lambda^2(q) < \lambda^2(q_r)$ and must lie on the solid portion of the integral curve for r^2 sketched through q_r in Figure 13.15(a). For the data shown in this figure, there is a state q_m that can be connected to both q_l and q_r by physically correct rarefaction waves, and the Riemann solution consists of two rarefactions as illustrated in Figure 13.14.

For other data this might not be the case. Figure 13.15(b) shows the data for the dam-break Riemann problem of Example 13.4, with $h_l = 3$, $h_r = 1$, and $u_l = u_r = 0$. We can still use (13.56) to compute an intermediate state q_m lying at the intersection of the integral curves, as illustrated in Figure 13.15(b), but the resulting 2-wave does not make physical sense as a rarefaction wave, since $\lambda^2(q_m) > \lambda^2(q_r)$. This wave would overturn, as illustrated in Figure 13.16.

Compare Figure 13.15(b) with Figure 13.10(b), where we found an all-shock solution to this same Riemann problem. In that case the 2-shock was acceptable, but the 1-shock failed to satisfy the entropy condition. The correct solution consists of a 1-rarefaction and a 2-shock as shown in Figure 13.5 and determined in the next section.

13.9 Solving the Dam-Break Problem

We now illustrate how to construct the general solution to a nonlinear Riemann problem, using the theory of shock waves and rarefaction waves developed above.

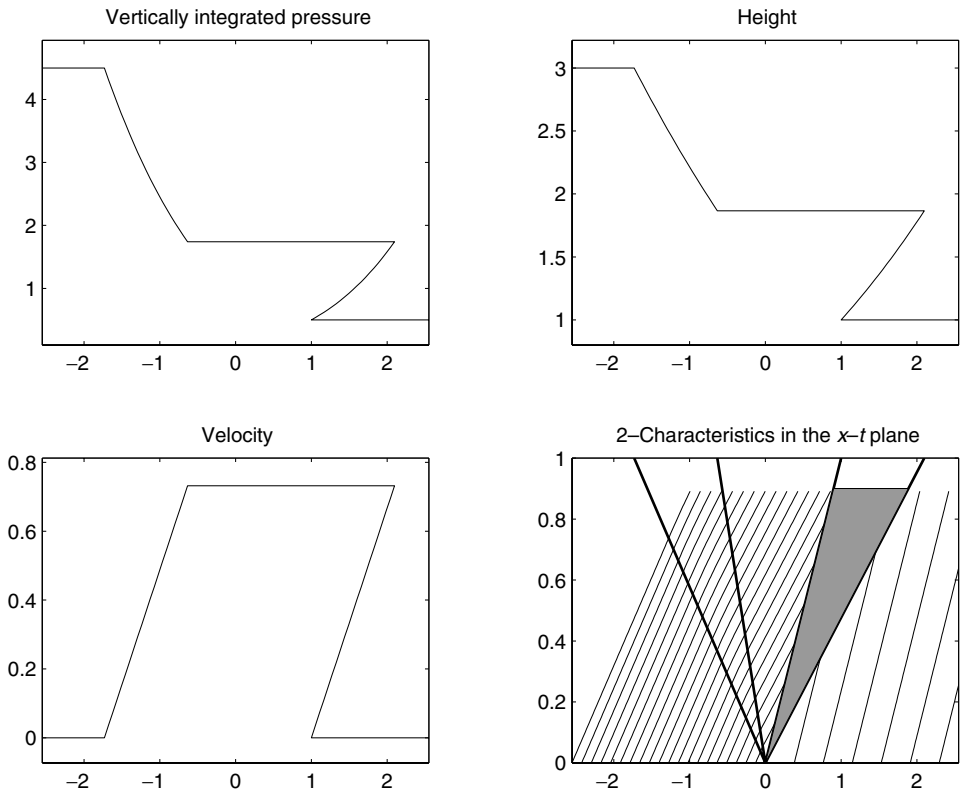

Fig. 13.16. Unphysical solution to the dam-break Riemann problem for the shallow water equations corresponding to the solution found in Figure 13.15(b). The 2-characteristics are shown in the lower right plot. Note that each point in the shaded region lies on three distinct 2-characteristics.

The dam-break Riemann problem for the shallow water equations (introduced in Example 13.4) has a solution that consists of a 1-rarefaction and a 2-shock, as illustrated in Figure 13.5. In Figure 13.10 we saw how to construct a weak solution to this problem that consists of two shock waves, one of which does not satisfy the Lax entropy condition. In Figure 13.15 we found an all-rarefaction solution to this problem that is not physically realizable. To find the correct solution we must determine an intermediate state q_m that is connected to q_l by a 1-rarefaction wave and simultaneously is connected to q_r by a 2-shock wave. The state q_m must lie on an integral curve of r^1 passing through q_l, so by (13.32) we must have

$$u_m = u_l + 2(\sqrt{gh_l} - \sqrt{gh_m}). \tag{13.57}$$

It must also lie on the Hugoniot locus of 2-shocks passing through q_r, so by (13.19) it must satisfy

$$u_m = u_r + (h_m - h_r)\sqrt{\frac{g}{2}\left(\frac{1}{h_m} + \frac{1}{h_r}\right)}. \tag{13.58}$$

We can easily eliminate u_m from these two equations and obtain a single nonlinear equation

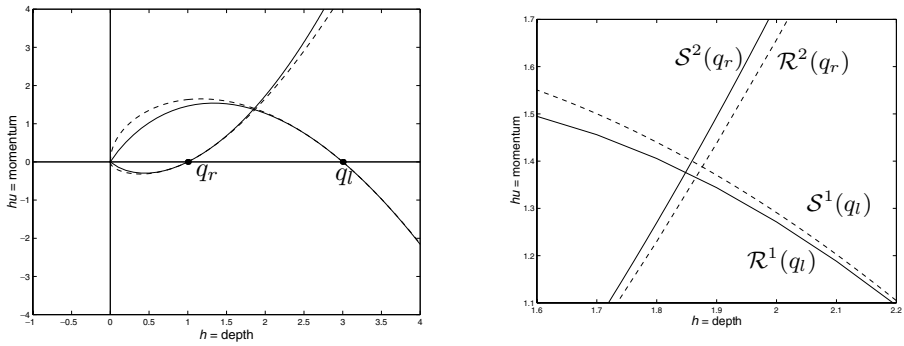

(a) (b)

Fig. 13.17. (a) The Hugoniot loci from Figure 13.10 together with the integral curves. (b) Close-up of the region where the curves intersect. $\mathcal{S}^1$: Entropy-violating 1-shocks; $\mathcal{R}^1$: 1-rarefactions; $\mathcal{S}^2$: 2-shocks; $\mathcal{R}^2$: unphysical 2-rarefactions.

to solve for h_m. The structure of the rarefaction wave connecting q_l to q_m can then be determined using the theory of Section 13.8.5.

Note that the intermediate state q_m resulting from this procedure will be slightly different from that obtained in either Figure 13.10 or Figure 13.15, since the Hugoniot loci are different from the integral curves. This is illustrated in Figure 13.17, where the curves from Figures 13.10 and 13.15 are plotted together. Figure 13.17(b) shows a close-up near the points of intersection of these curves. The correct solution to the dam-break Riemann problem has the intermediate state at the point where the two solid lines cross.

Note that both sets of curves are tangent to the eigenvector $r^1(q_l)$ at q_l and to $r^2(q_r)$ at q_r. Moreover, it can be shown that the Hugoniot locus and the integral curve through a given point have the same curvature at that point, and so the curves are really quite similar near that point. (See, e.g., Lax [263].) How rapidly the curves diverge from one another typically depends on how nonlinear the system is. For a linear system, of course, the integral curves and Hugoniot loci are identical, each being straight lines in the directions of the constant eigenvectors. Even for nonlinear systems the Hugoniot loci *may* be identical to the integral curves, though this is not the usual situation. See Exercise 13.12 for one example, and Temple [447] for some general discussion of such systems, which are often called *Temple-class systems*.

13.10 The General Riemann Solver for Shallow Water Equations

For the dam-break problem we know that the 1-wave is a rarefaction while the 2-wave is a shock, leading to the system of equations (13.57) and (13.58) to solve for h_m and u_m. For general values of q_l and q_r we might have any combination of shocks and rarefactions in the two families, depending on the specific data. To find the state q_m in general we can define two functions ϕ_l and ϕ_r by

$$\phi_l(h) = \begin{cases} u_l + 2(\sqrt{gh_l} - \sqrt{gh}) & \text{if } h < h_l, \\ u_l - (h - h_l)\sqrt{\frac{g}{2}\left(\frac{1}{h} + \frac{1}{h_l}\right)} & \text{if } h > h_l, \end{cases}$$

and

$$\phi_r(h) = \begin{cases} u_r - 2(\sqrt{gh_r} - \sqrt{gh}) & \text{if } h < h_r, \\ u_r + (h - h_r)\sqrt{\frac{g}{2}\left(\frac{1}{h} + \frac{1}{h_r}\right)} & \text{if } h > h_r. \end{cases}$$

For a given state h, the function $\phi_l(h)$ returns the value of u such that (h, hu) can be connected to q_l by a physically correct 1-wave, while $\phi_r(h)$ returns the value such that (h, hu) can be connected to q_r by a physically-correct 2-wave. We want to determine h_m so that $\phi_l(h_m) = \phi_r(h_m)$. This can be accomplished by applying a nonlinear root finder to the function $\phi(h) \equiv \phi_l(h) - \phi_r(h)$.

13.11 Shock Collision Problems

In a scalar equation, such a Burgers equation, when two shock waves collide, they simply merge into a single shock wave with a larger jump. For a system of equations, the result of a shock collision is not so simple, even if the two shocks are in the same characteristic family. The result will include a stronger shock in this same family, but the collision will typically also introduce waves in the other families. For example, consider initial data for the shallow water equations consisting of the three states shown in Figure 13.18(a). These three states all lie on the Hugoniot locus $\mathcal{S}^2(q_2)$, so there is a 2-shock connecting q_1 to q_2 and a slower 2-shock connecting q_2 to q_3. (Note that the shock speed $s = [\![hu]\!]/[\![h]\!]$ is given by the slope of the line joining the two points.) If we solve the shallow water equations with data

$$q(x, 0) = \begin{cases} q_1 & \text{if } x < x_1, \\ q_2 & \text{if } x_1 \le x \le x_2, \\ q_3 & \text{if } x > x_2 \end{cases} \tag{13.59}$$

for some initial shock locations $x_1 < x_2$, then the solution consists of the these two shocks, which eventually collide at some point x_c. At the time t_c when they collide, the state q_2

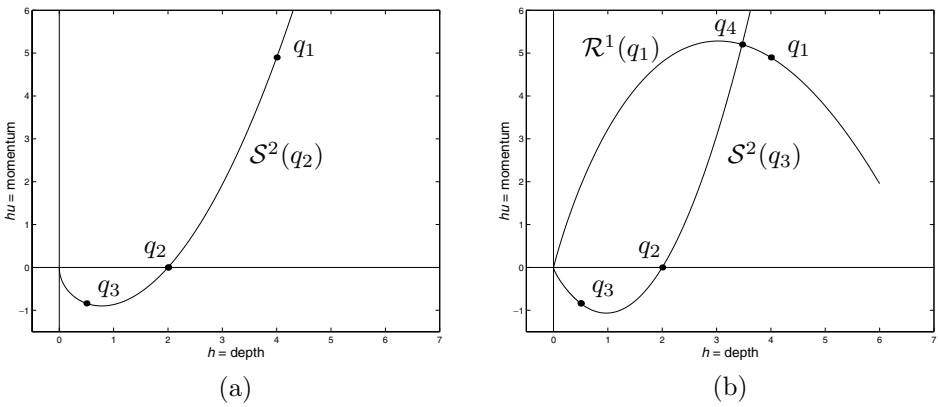

Fig. 13.18. States arising in the collision of two 2-shocks for the shallow water equations. (a) Initial states q_1 and q_3 are each connected to q_2 by a 2-shock. (b) After collision, solving the Riemann problem between q_3 and q_1 gives a new state q_4 and a reflected 1-wave.

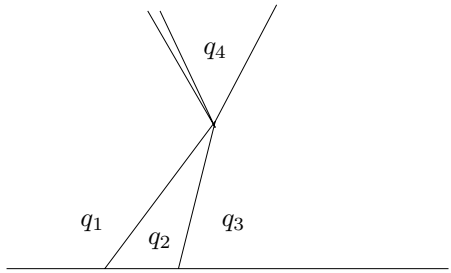

Fig. 13.19. Collision of two 2-shocks giving rise to a 1-rarefaction and a 2-shock, as seen in the x–t plane.

disappears and the solution has the form

$$q(x, t_c) = \begin{cases} q_1 & \text{if } x < x_c, \\ q_3 & \text{if } x > x_c. \end{cases} \tag{13.60}$$

To determine the solution beyond this time, note that this has the form of Riemann-problem data with left state q_1 and right state q_3. The Riemann solution is not a single 2-shock, because q_1 will not lie on the Hugoniot locus $\mathcal{S}^2(q_3)$. Instead, a 1-wave must be introduced to connect q_1 to a new state q_4 that lies on this Hugoniot locus, as illustrated in Figure 13.18(b). We see that the 1-wave must be a rarefaction wave, since $h_4 < h_1$ and h_4 is determined by the intersection of the integral curve $\mathcal{R}^1(q_1)$ with the Hugoniot locus $\mathcal{S}^2(q_3)$. (Note that q_2 does lie on the Hugoniot locus $\mathcal{S}^2(q_3)$, since q_3 lies on the Hugoniot locus $\mathcal{S}^2(q_2)$.)

A view of this collision in the x–t plane is seen in Figure 13.19. To view a numerical solution of this collision, see `[claw/book/chap13/collide]`.

13.12 Linear Degeneracy and Contact Discontinuities

The shallow water equations are a system of two equations for which both characteristic fields are genuinely nonlinear, as defined in Section 13.8.4. A smooth simple wave in one of these fields will always distort via compression or expansion as characteristics converge or diverge. For the Riemann problem, each wave will be either a single shock or a rarefaction wave. Genuine nonlinearity of the pth field requires that the eigenvalue λ^p be monotonically varying as we move along an integral curve of r^p, and hence that $\nabla\lambda^p(q) \cdot r^p(q)$ be nonzero everywhere.

We now consider the opposite extreme, a field in which $\nabla\lambda^p(q) \cdot r^p(q)$ is identically zero for all q, so that λ^p is constant along each integral curve of r^p (but may take different values on different integral curves). Such a field is called *linearly degenerate*, since simple waves in which the variation of q is only in this field behave like solutions to linear hyperbolic equations. Since λ^p is constant throughout the wave, it simply translates with this constant speed without distorting. If the initial data is a jump discontinuity, with q_l and q_r both lying on a single integral curve of this field, then the solution will consist of this discontinuity propagating at the constant speed λ^p associated with this integral curve. Hence the Hugoniot locus for this field agrees with the integral curve. Such a discontinuity is not a shock

wave, however, since the characteristic speed $\lambda^p(q_l) = \lambda^p(q_r)$ on each side agrees with the propagation speed of the wave. Characteristics are parallel to the wave in the x–t plane rather than impinging on it. Waves of this form are generally called *contact discontinuities*, for reasons that will become apparent after considering the simple example in the next section.

13.12.1 Shallow Water Equations with a Passive Tracer

Again consider the shallow water equations, but now suppose we introduce some dye into the water in order to track its motion. Let $\phi(x, t)$ represent the concentration of this passive tracer, measured in units of mass or molarity per unit volume, so that it is a *color* variable as described in Chapter 9. Then values of ϕ move with the fluid velocity u and are constant along particle paths, and ϕ satisfies the color equation (9.12),

$$\phi_t + u\phi_x = 0. \tag{13.61}$$

Since ϕ measures a passive tracer that is assumed to have no influence on the fluid dynamics, it simply satisfies this linear advection equation with the variable coefficient $u(x, t)$, which can be obtained by first solving the shallow water equations. However, to illustrate linearly degenerate fields we can couple this equation into the shallow water equations and obtain an augmented system of three conservation laws.

We first rewrite (13.61) as a conservation law by instead considering the conserved quantity $h\phi W$, where h is the depth of the water and W is the width of the channel modeled in our one-dimensional equations. This is needed solely for dimensional reasons, and we can take $W = 1$ in the appropriate length units and consider $h\phi$ as the conserved quantity, measuring mass or molarity per unit length. This is conserved in one dimension with the flux $uh\phi$, so $h\phi$ satisfies the conservation law

$$(h\phi)_t + (uh\phi)_x = 0. \tag{13.62}$$

Note that differentiating this out gives

$$h_t\phi + h\phi_t + (hu)_x\phi + (hu)\phi_x = 0,$$

and using $h_t + (hu)_x = 0$ allows us to relate this to the color equation (13.61). Numerically one can work directly with (13.61) rather than (13.62) since the wave-propagation algorithms do not require that all equations be in conservation form, and there are often advantages to doing so (see Section 16.5).

For our present purposes, however, we wish to investigate the mathematical structure of the resulting system of conservation laws. Augmenting the shallow water equations with (13.62) gives the system $q_t + f(q)_x = 0$ with

$$q = \begin{bmatrix} h \\ hu \\ h\phi \end{bmatrix} = \begin{bmatrix} q^1 \\ q^2 \\ q^3 \end{bmatrix}, \qquad f(q) = \begin{bmatrix} hu \\ hu^2 + \frac{1}{2}gh^2 \\ uh\phi \end{bmatrix} = \begin{bmatrix} q^2 \\ (q^2)/q^1 + \frac{1}{2}g(q^1)^2 \\ q^2q^3/q^1 \end{bmatrix}. \tag{13.63}$$

The Jacobian is now

$$f'(q) = \begin{bmatrix} 0 & 1 & 0 \\ -(q^1)^2/(q^1)^2 + gq^1 & 2q^2/q^1 & 0 \\ -q^2q^3/(q^1)^2 & q^3/q^1 & q^2/q^1 \end{bmatrix} = \begin{bmatrix} 0 & 1 & 0 \\ -u^2 + gh & 2u & 0 \\ -u\phi & \phi & u \end{bmatrix}. \quad (13.64)$$

This is a block lower-triangular matrix, and the eigenvalues are given by those of the two blocks. The upper 2×2 block is simply the Jacobian matrix (13.8) for the shallow water equations, and has eigenvalues $u \pm \sqrt{gh}$. The lower 1×1 block yields the additional eigenvalue u. The eigenvectors are also easy to compute from those of (13.8), and we find that

$$\begin{aligned} \lambda^1 &= u - \sqrt{gh}, & \lambda^2 &= u, & \lambda^3 &= u + \sqrt{gh}, \\ r^1 &= \begin{bmatrix} 1 \\ u - \sqrt{gh} \\ \phi \end{bmatrix}, & r^2 &= \begin{bmatrix} 0 \\ 0 \\ 1 \end{bmatrix}, & r^3 &= \begin{bmatrix} 1 \\ u + \sqrt{gh} \\ \phi \end{bmatrix}. \end{aligned} \quad (13.65)$$

The fact that the scalar ϕ is essentially decoupled from the shallow water equations is clearly apparent. Fields 1 and 3 correspond to the nonlinear waves in the shallow water equations and involve ϕ only because the conserved quantity $h\phi$ has a jump discontinuity where there is a jump in h. The tracer concentration ϕ is continuous across these waves. Field 2 carries a jump in ϕ alone, since the first two components of r^2 are 0. The speed of the 2-wave, $\lambda^2 = u$, depends on the shallow water behavior, just as we expect.

If we considered very small variations in h and u, we could linearize this system and obtain a form of the acoustics equations coupled with the advection equation for ϕ. This linear system has already been considered in Section 3.10 and shows the same basic structure.

For the nonlinear system, fields 1 and 3 are still genuinely nonlinear, as in the standard shallow water equations, but field 2 is linearly degenerate, since it corresponds to the linear advection equation. This is easily verified by computing

$$\nabla\lambda^2 = \begin{bmatrix} -u/h \\ 1/h \\ 0 \end{bmatrix}$$

and observing that $\nabla\lambda^2 \cdot r^2 \equiv 0$. (Recall that $\nabla\lambda^2$ means the gradient of $u = (hu)/h = q^2/q^1$ with respect to q.)

Any variation in ϕ will simply be advected with velocity u. In general the shape of ϕ may distort, since $u(x, t)$ may vary in the solution to the shallow water equations. However, if we consider a simple wave in Field 2, then variations in q can occur only along an integral curve of r^2. This vector always points in the ϕ-direction in the three-dimensional state space, and integral curves are straight lines in this direction with no variation in h or hu. So in particular u is constant along any integral curve of r^2, and simple waves consist of arbitrary variations in ϕ being carried along in water of constant depth moving at constant speed u. These are, of course, special solutions of the augmented shallow water equations.

13.12.2 The Riemann Problem and Contact Discontinuities

Now consider the Riemann problem for the augmented shallow water system (13.63), with piecewise constant data having an arbitrary jump between states q_l and q_r (which allows arbitrary jumps in h, u, and ϕ). It is clear how to solve this Riemann problem. Since ϕ does not affect h or u, the procedure of Section 13.9 can be used to determine the 1-wave and 3-wave. Each is a shock or rarefaction wave, as in the standard shallow water equations, and there is no variation in ϕ across either of these waves. The 1-wave is moving into the fluid on the left, in which $\phi \equiv \phi_l$ while the 3-wave is moving into the fluid on the right, in which $\phi \equiv \phi_r$. Between these two waves the velocity u_m is constant (obtained as in Section 13.9), and a 2-wave is now introduced with velocity $\lambda^2 = u_m$. Across this wave, $h = h_m$ and $u = u_m$ are constant while ϕ jumps from ϕ_l to ϕ_r. This wave has a simple physical interpretation: it marks the boundary between water that was initially to the left of the interface and water that was initially to the right. This is clear because ϕ satisfies the color equation and hence is constant on particle paths.

This 2-wave is called a *contact discontinuity* because it marks the point at which the two distinct fluids (e.g., with different colors) are in contact with one another. Figure 13.20

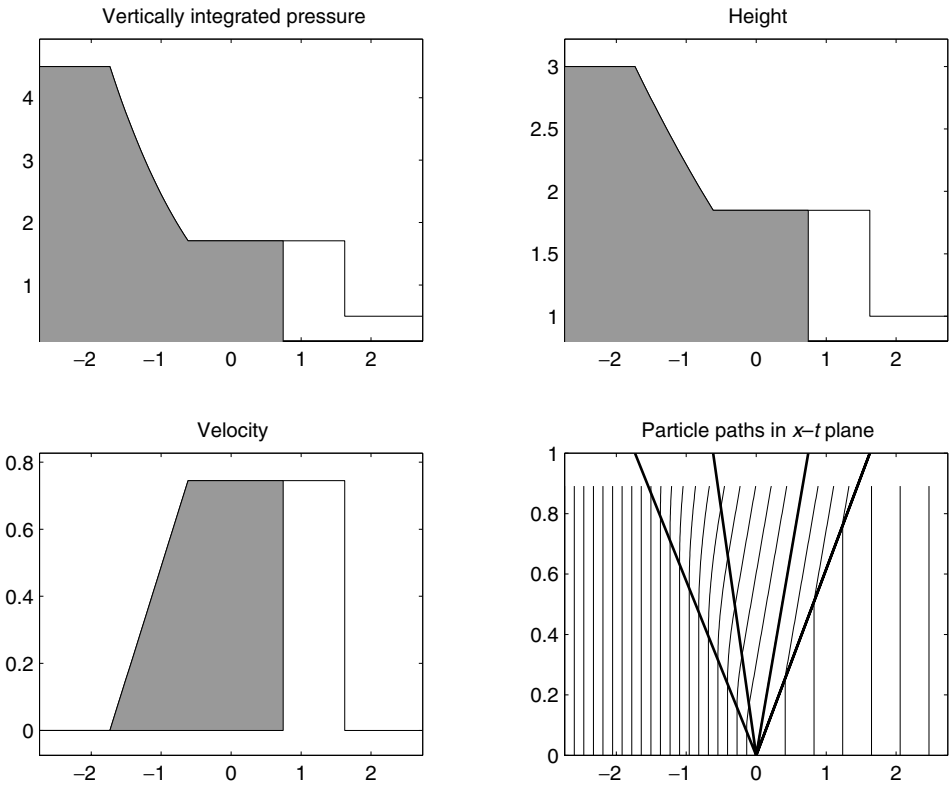

Fig. 13.20. Structure of the similarity solution of the dam-break Riemann problem for the augmented shallow water equations with $u_l = u_r = 0$. The depth h, velocity u, and vertically integrated pressure are displayed as functions of x/t. The value of ϕ is indicated by coloring the water darker where $\phi = \phi_l$. The structure in the x–t plane is also shown, and particle paths are indicated for a set of particles with the spacing between particles inversely proportional to the depth. The contact discontinuity is now indicated along with the rarefaction and shock.

shows one example for the dam-break problem of Example 13.4. This looks exactly like Figure 13.5 except that we have now also indicated the variation in ϕ by coloring the water that was initially behind the dam (i.e., in the region $x < 0$) darker. The contact discontinuity is indicated in the plot of particle paths, and it is clear that this wave separates water initially behind the dam from water initially downstream.

Since the characteristic velocity $\lambda^2 = u$ agrees with the particle velocity, we can also interpret this plot of particle paths as a plot of the 2-characteristics for the augmented system. These characteristics cross the 1-wave and 3-wave and are parallel to the 2-wave, as expected because this field is linearly degenerate.

The Euler equations of gas dynamics, discussed in the next chapter, also have a linearly degenerate field corresponding to contact discontinuities. For general initial data the Riemann solution may contain a jump in density across the surface where the two initial gases are in contact.

Exercises

13.1. (a) Consider an integral curve of r^1 for the shallow water equations, as illustrated in Figure 13.13(a), for example. Show that the slope tangent to this curve in the q^1–q^2 plane at any point is equal to λ^1 at that point. ($q^1 = h$ and $q^2 = hu$.)

(b) Consider the Hugoniot locus for 1-shocks for the shallow water equations, as illustrated in Figure 13.9(a), for example. Show that if q_l and q_r are two points lying on this curve (and hence connected by a 1-shock) then the slope of the secant line connecting these points is equal to the shock speed s.

13.2. The graphs of Figure 13.15 show the h–hu plane. The curves look somewhat different if we instead plot them in the h–u plane.

(a) Redraw Figure 13.15(a) in the h–u plane.

(b) Draw a similar figure for $h_l = h_r = 1$ and $-u_l = u_r = 1.9$.

(c) Draw a similar figure for $h_l = h_r = 1$ and $-u_l = u_r = 2.1$. In this case the Riemann solution contains a region in which $h = 0$: dry land between the two outgoing rarefaction waves.

13.3. Repeat the computations of Example 13.9 to determine the form of 2-rarefactions in the shallow water equations and show that this field is genuinely nonlinear.

13.4. For the shallow water equations, show that when a 1-shock collides with a 2-shock the result is a new pair of shocks. Exhibit the typical solution in the phase plane and the x–t plane.

13.5. In the shallow water equations, is it possible for two 2-rarefactions to collide with each other?

13.6. For the shallow water equations, the total energy can be used as an entropy function in the mathematical sense. This function and the associated entropy flux are given by

$$\begin{aligned} \eta(q) &= \frac{1}{2}hu^2 + \frac{1}{2}gh^2, \\ \psi(q) &= \frac{1}{2}hu^3 + gh^2u. \end{aligned} \tag{13.66}$$

Verify this by showing the following.

(a) $\eta(q)$ is convex: Show that the Hessian matrix $\eta''(q)$ is positive definite.
(b) $\eta(q)_t + \psi(q)_x = 0$ for smooth solutions: Verify that (11.47) holds, $\psi'(q) = \eta'(q)f'(q)$.

13.7. Consider the p-system (described in Section 2.13),

$$\begin{aligned} v_t - u_x &= 0, \\ u_t + p(v)_x &= 0, \end{aligned}$$

where $p(v)$ is a given function of v.
(a) Compute the eigenvalues of the Jacobian matrix, and show that the system is hyperbolic provided $p'(v) < 0$.
(b) Use the Rankine–Hugoniot condition to show that a shock connecting $q = (v, u)$ to some fixed state $q^* = (v^*, u^*)$ must satisfy

$$u = u_* \pm \sqrt{-\left(\frac{p(v) - p(v_*)}{v - v_*}\right)}(v - v_*). \tag{13.67}$$

(c) What is the propagation speed for such a shock? How does this relate to the eigenvalues of the Jacobian matrix computed in part (a)?
(d) Plot the Hugoniot loci for the point $q_* = (1, 1)$ over the range $-3 \le v \le 5$ for each of the following choices of $p(v)$. (Note that these are not physically reasonable models for pressure as a function of specific volume!)
  (i) $p(v) = -e^v$,
  (ii) $p(v) = -(2v + 0.1e^v)$,
  (iii) $p(v) = -2v$.
(e) Determine the two-shock solution to the Riemann problem for the p-system with $p(v) = -e^v$ and data

$$q_l = (1, 1), \qquad q_r = (3, 4).$$

Do this in two ways:
  (i) Plot the relevant Hugoniot loci, and estimate where they intersect.
  (ii) Set up and solve the proper scalar nonlinear equation for v_m. You might use the Matlab command `fzero` or write your own Newton solver.
(f) Does the Riemann solution found in the previous part satisfy the Lax entropy condition? Sketch the structure of the solution in the x–t plane, showing also some sample 1-characteristics and 2-characteristics.
(g) For the given left state $q_l = (1, 1)$, in what region of the phase plane must the right state q_r lie in order for the two-shock Riemann solution to satisfy the Lax entropy condition?

13.8. Consider the p-system of Exercise 13.7, and take $p(v) = -e^v$.
(a) Follow the procedure of Section 13.8.1 to show that along any integral curve of r^1 the relation

$$u = u_* - 2\left(e^{v_*/2} - e^{v/2}\right)$$

must hold, where (v_*, u_*) is a particular point on the integral curve. Conclude that

$$w^1(q) = u - 2e^{v/2}$$

is a 1-Riemann invariant for this system.

(b) Follow the procedure of Section 13.8.5 to show that through a centered rarefaction wave

$$\tilde{u}(\xi) = A - 2\xi,$$

where

$$A = u_l - 2e^{v_l/2} = u_r - 2e^{v_r/2},$$

and determine the form of $\tilde{v}(\xi)$.

(c) Show that this field is genuinely nonlinear for all q.

(d) Determine the 2-Riemann invariants and the form of a 2-rarefaction.

(e) Suppose arbitrary states q_l and q_r are specified and we wish to construct a Riemann solution consisting of two "rarefaction waves" (which might not be physically realizable). Determine the point $q_m = (v_m, u_m)$ where the two relevant integral curves intersect.

(f) What conditions must be satisfied on q_l and q_r for this to be the physically correct solution to the Riemann problem?

13.9. For the general p-system of Exercise 13.7, determine the condition on the function $p(v)$ that must be satisfied in order for both fields to be genuinely nonlinear for all q.

13.10. Consider the equations (2.97) modeling a one-dimensional slice of a nonlinear elastic solid. Suppose the stress–strain relation $\sigma(\epsilon)$ has the shape indicated in Figure 2.3(a). Is the system genuinely nonlinear in this case?

13.11. The variable-coefficient scalar advection equation $q_t + (u(x)q)_x = 0$ studied in Section 9.4 can be viewed as a hyperbolic system of two equations,

$$\begin{aligned} q_t + (uq)_x &= 0, \\ u_t &= 0, \end{aligned} \tag{13.68}$$

where we now view $u(x, t) \equiv u(x)$ as a second component of the system.

(a) Determine the eigenvalues and eigenvectors of the Jacobian matrix for this system.

(b) Show that both fields are linearly degenerate, and that in each field the integral curves and Hugoniot loci coincide. Plot the integral curves of each field in the q–u plane.

(c) Indicate the structure of a general Riemann solution in the q–u plane for the case $u_l, u_r > 0$. Relate this to Figure 9.1.

(d) Note that this system fails to be strictly hyperbolic along $u = 0$. Can the Riemann problem be solved if $u_l < 0$ and $u_r > 0$? If $u_l > 0$ and $u_r < 0$? (See Section 16.4.2 for more discussion of such problems.)

13.12. Consider the system

$$\begin{aligned} v_t + [vg(v,\phi)]_x &= 0, \\ \phi_t + [\phi g(v,\phi)]_x &= 0, \end{aligned} \tag{13.69}$$

where $g(v, \phi)$ is a given function. Systems of this form arise in two-phase flow. As a simple example, take $g(v, \phi) = \phi^2$ and assume $\phi > 0$.

(a) Determine the eigenvalues and eigenvectors for this system and show that the first field is linearly degenerate while the second field is genuinely nonlinear.

(b) Show that the Hugoniot locus of any point q_* consists of a pair of straight lines, and that each line is also the integral curve of the corresponding eigenvector.

(c) Obtain the general solution to the Riemann problem consisting of one shock and one contact discontinuity. Show that this solution satisfies the Lax Entropy Condition 11.1 if and only if $\phi_l \geq \phi_r$.